

Investigating Carbonyl Compounds above the Amazon Rainforest using PTR-ToF-MS with NO⁺ Chemical Ionization

Akima Ringsdorf¹, Achim Edtbauer¹, Bruna Holanda², Christopher Poehlker², Marta O. Sá³, Alessandro Araújo⁴, Jürgen Kesselmeier², Jos Lelieveld^{1,5}, Jonathan Williams^{1,5}

¹Department of Atmospheric Chemistry, Max Planck Institute for Chemistry, Mainz, Germany

²Department of Multiphase Chemistry, Max Planck Institute for Chemistry, Mainz, Germany

³Instituto Nacional de Pesquisas da Amazonia (INPA), Manaus, CEP 69067-375, Brazil

⁴Empresa Brasileira de Pesquisa Agropecuária (Embrapa) Amazonia Oriental, Belem, CEP 66095-100, Brazil

⁵Climate and Atmosphere Research Center, The Cyprus Institute, 1645 Nicosia, Cyprus

Correspondence to: Jonathan Williams (J.Williams@mpic.de) and Akima Ringsdorf (A.Ringsdorf@mpic.de)

Abstract. The photochemistry of carbonyl compounds significantly influences tropospheric chemical composition by altering the local oxidative capacity, free radical abundance in the upper troposphere, and formation of ozone, PAN, and secondary organic aerosol particles. Carbonyl compounds can be emitted directly from the biosphere into the atmosphere and are formed through photochemical degradation of various precursor compounds. Aldehydes have atmospheric lifetimes of hours to days, in contrast to ketones, which persist for up to several weeks. While standard operating conditions for proton transfer time-of-flight mass spectrometer (PTR-ToF-MS) using H₃O⁺ ions are unable to separate aldehydes and ketones, the use of NO⁺ reagent ions allows for the differential detection of isomeric carbonyl compounds with a high time resolution. Here we study the temporal (24 h) and vertical (80–325 m) variability of individual carbonyl compounds in the Amazon rainforest atmosphere with respect to their rainforest-specific sources and sinks. We found strong sources of ketones within or just above the rainforest canopy (acetone, MEK, and C₅-ketones). A common feature of the carbonyls was nocturnal deposition observed by loss rates, most likely since oxidized volatile organic compounds are rapidly metabolized and utilized by the biosphere. With NO⁺ chemical ionization, we show that the dominant carbonyl species include acetone and propanal, which are present at a ratio of 1:10 in the wet-to-dry transition and 1:20 in the dry season.

1 Introduction

On a global scale, tropical forests are regarded as the largest source of biogenic volatile organic compounds (BVOC) for the atmosphere (Guenther, 2013). BVOC comprise multiple compound classes including terpenes, alkenes, alkanes, alcohols, acids, esters, halocarbons, and carbonyls, all emitted as a result of various physiological processes, such as those occurring in plants, soils, etc., and as a function of environmental conditions. The emission quantity and composition vary among plant species, thus given the high biodiversity in tropical forests, the ecosystem composition and developmental stage also need to be considered as clearly demonstrated by Ciccioli et al. (2023). Most of the carbon released as BVOC from the tropical rainforest is in the form of terpenes, including the hemiterpene isoprene (C₅H₈) (Yáñez-Serrano et al., 2015), monoterpenes such as alpha-pinene (C₁₀H₁₆) (Zannoni et al., 2020b), and sesquiterpenes such as copaene (C₁₅H₂₄) (Yee et al., 2020). In addition, considerable amounts of oxygenated VOC (OVOC) are known to be present in rainforest air, with carbonyl compounds, namely aldehydes and ketones containing the C=O functional group, constituting an important subset of the atmospheric OVOC (Kesselmeier and Staudt, 1999). Direct biogenic emission, biomass burning, and secondary formation, mainly from the oxidation of the aforementioned terpene precursors and photolysis of larger carbonyls, all contribute to the cocktail of carbonyl compounds in the atmosphere (Guenther, 2013; Liu et al., 2022; Mellouki et al., 2015). To understand this cocktail, deposition and uptake by vegetation, i.e., bidirectional exchange, should always be considered as potential contributors (Kesselmeier, 2001; Kesselmeier et al., 1997; Villanueva et al., 2014). The formation of carbonyl species occurs after the oxidation of VOC is initiated by the hydroxyl radical (OH), ozone (O₃), or at nighttime by the nitrate radical (NO₃), and the resulting peroxy radicals (RO₂) react either with nitrogen oxide (NO) (when present) or with other ambient RO₂ or

45 HO₂ radicals. In the presence of NO this oxidation chain results in a net production of O₃, an important radiatively
46 active oxidant in the Amazon and worldwide (Mellouki et al., 2015; Trebs et al., 2012).

47 The main atmospheric carbonyl sinks are photolysis and oxidation by OH (Atkinson and Arey, 2003). As a
48 consequence, reactions with carbonyls combined with those of other BVOC determine the availability of OH and thus
49 the oxidative capacity of the atmosphere (Lelieveld et al., 2016). In Amazon rainforest air, OVOC account for 22-40 %
50 of OH reactivity, namely the overall loss frequency of OH radicals (Pfannerstill et al., 2021). Unsaturated carbonyls,
51 like the isoprene oxidation products methacrolein (MACR) and methyl vinyl ketone (MVK), are also oxidized by O₃.
52 Ketones, such as acetone, react much less readily with OH than aldehydes and, accordingly, have longer atmospheric
53 lifetimes. Thus, they persist during long-range transport and convective lifting to high altitudes, whereas more reactive
54 aldehydes impact the chemistry more locally. However, through rapid, deep convection, a frequent phenomenon in
55 the humid and hot tropics, also aldehydes can be transported to altitudes between 10 and 17 km (Prather and Jacob,
56 1997).

57 Oxidation of aldehydes and photolysis of ketones and dicarbonyls and further reaction with NO_x (NO + NO₂) yields
58 peroxydicarboxylic nitric anhydride (PAN). PAN and other peroxydicarboxylics are thermally unstable near the surface but
59 in the cooler mid- and upper troposphere PAN is the most abundant reservoir for nitrogen oxides and is transported
60 over long distances (Mellouki et al., 2015; Fischer et al., 2014; Singh et al., 1990; Roberts, 2007). The main precursors
61 of PAN are acetaldehyde, followed by more minor contributions from methylglyoxal (not reported here) and acetone
62 (Fischer et al., 2014). NO_x in the tropical atmosphere originates from several processes, starting with microbial
63 activities in soils and the release of NO, which is rapidly oxidized to NO₂, a large fraction even before it escapes the
64 canopy. NO₂ can be taken up by vegetation and only a part of this species traverses the canopy to the atmosphere
65 above (Breuninger et al., 2013; Chaparro-Suarez et al., 2011; Rummel et al., 2002). Further sources are lightning
66 discharges and biomass burning, the latter having the strongest seasonal variability (Bond et al., 2002).

67 The photochemical degradation of carbonyls in the atmosphere is also a source of HO_x (HO₂ + OH) radicals,
68 particularly important in the upper troposphere where OH radical production from carbonyls can exceed primary
69 production in areas impacted by convection (Colomb et al., 2006; Lary and Shallcross, 2000; Liu et al., 2022; Prather
70 and Jacob, 1997). Furthermore, the abundance of radicals and oxidation products of carbonyls and dicarbonyls can
71 promote the formation and growth of secondary organic aerosols (Liu et al., 2022).

72 In this study, the observed diel and vertical (80-325 m) variability of 15 carbonyl species (C₂-C₉) was investigated.
73 These species were detected online with a PTR-ToF-MS using NO⁺ as a reagent ion. This technique enables the
74 separation of isomeric aldehydes and ketones to identify their partitioning in the Amazonian atmospheric boundary
75 layer (ABL) at the ATTO site. Previous measurements of carbonyls have been conducted over the rainforest using
76 PTR-MS with H₃O⁺ as the reagent ion (Yáñez-Serrano et al., 2016). With this method, both aldehyde and ketone
77 carbonyl forms are detected at the same mass. Usually, for airborne measurements, atmospheric chemists have argued
78 that the m/z used for the detection of C₃ carbonyls can be interpreted to be predominantly acetone since its atmospheric
79 lifetime is relatively long (Williams et al., 2001). However, near biogenic sources, the fractional distribution can be
80 different, and especially if the data is used to extract further information about the environment, such as OH
81 concentrations (Williams et al., 2000), the validity of this assumption should be verified.

82 The dataset presented here is the first online measurement of speciated individual aldehydes and ketones in the
83 Amazon. This rainforest environment is characterized by high solar insolation and vigorous vertical transport by deep
84 convection. In quantifying the relative abundance of carbonyl species, we aimed to improve the understanding of their
85 emissions, secondary formation in the atmosphere, transformation, and deposition in the Amazon rainforest region.

86 **2 Experimental**

87 **2.1 Measurement site and instrumentation**

88 All measurements were conducted at the Amazon Tall Tower Observatory (ATTO) within the primary tropical
89 rainforest of Brazil. The site is located 135 km NE of Manaus (02.14°S, 58.99°W, 120 m above sea level) with the
90 main wind direction being NE to SE (Fig. S1). In the wet season (February–May), the air is typically nearly pristine

91 since the air masses pass over more than 1000 km of mostly unperturbed rainforest before being sampled, with a
92 possible influence due to long-range transport from African biomass burning pollution, which has been observed in
93 the beginning of the dry season (February–March) (Holanda et al., 2023). This is reflected by low concentrations of
94 NO_x of less than 150 ppt in the ABL during the late wet season. In the dry season (August–November), however, air
95 influenced by mainly man-made biomass burning in South America was observed. In the same season enhanced black
96 carbon concentrations were measured due to the hemispheric wide summer maximum in biomass burning. The site
97 hosts a 325–m–tall tower and an 80–m walk-up tower, among other measurement and accommodation facilities. A
98 detailed map can be found in the Supplement (Fig. S2). The canopy height of the surrounding forest is about 35 m
99 (Kuhn et al., 2007). A comprehensive description of the site is provided by Andreae et al. (2015). The measurements
100 described here were conducted from June 23 until July 8 and from September 27 until October 14, 2019.

101 The sampling inlets for the BVOC measurements are located at 80, 150, and 325 m on the tall tower. Air is drawn by
102 high-volume pumps down to the instrumentation that is stored in an air-conditioned container at the foot of the tower.
103 By sequentially sampling each height for 5 minutes, a semi-continuous measurement can be achieved, so that each
104 height is sampled four times per hour. The flow in the insulated and heated (40 °C) Teflon sampling lines (3/8"OD)
105 is about 10 l min⁻¹. A long inlet line can be compared to a gas chromatographic column, which retains the sampled
106 VOC depending on their volatility and polarity, expressed by a wall saturation concentration (Pagonis et al., 2017).
107 ~~Adsorption to~~The flow through the ~~the 325 m inner walls of the~~ Teflon line caused a response time of 90 seconds at
108 ATTO using a VOC gas standard. Before the actual sampling of each height, the line was ~~therefore~~ flushed with
109 ambient air to achieve saturation. Tests with a 400–m inlet line in China have shown that the carbonyl compounds
110 investigated in this study have high saturation concentrations (C*, which is inversely proportional to the wall
111 partitioning) and are not affected by line loss (Deming et al., 2019; Li et al., 2023), but line effects such as a broadening
112 of initially sharp concentration peaks cannot be excluded. It has to be noted that sharp concentration peaks or spikes
113 of short duration (< 90 s) were not expected high above the homogenous vegetation of the rainforest. Some less
114 volatile molecules, like sesquiterpenes, never reached saturation and were additionally potentially degraded by O₃ or
115 NO₃ (which was shown to form inside the insulated tubing (Li et al., 2023)); thus, they were not detected. A potential
116 contribution from the oxidation of sesquiterpenes inside the tubing to detected carbonyl species cannot be excluded;
117 however, this contribution is expected to be minor given the rapidly decreasing sesquiterpene concentrations with
118 increasing distance from the canopy (Yee et al., 2018). The residence time in the tubing is short compared to the time
119 that sesquiterpenes are exposed to oxidation during atmospheric transport before reaching the sampling heights. VOC
120 were measured by a Proton Transfer Reaction Time of Flight Mass Spectrometer (PTR-ToF-MS 4000, Ionicon
121 Analytik, Innsbruck, Austria) (Jordan et al., 2009) with a time resolution of 20 seconds and averaged to 4 minutes.

122 Meteorological data were measured at the walk-up tower at multiple heights up to 80 m (LI7500A, LI-COR
123 Biotechnology, Lincoln, USA) and at the tall tower at 325 m (Lufft, WS600-LMB, G. Lufft Mess- und Regeltechnik
124 GmbH, Fellbach, Germany) with a time resolution of 1 minute.

125

126 2.2 NO+ chemical ionization

127 PTR-ToF-MS in general is a form of chemical ion mass spectrometry (CIMS) commonly operated with hydronium
128 ions (H₃O⁺) for the chemical ionization of VOC in air samples. The technique is well-established and sensitive and is
129 able to detect most of the prominent VOC in ambient air with a high temporal resolution of seconds (de Gouw and
130 Warneke, 2007). The proton transfer reaction that lends its name to the instrument occurs between H₃O⁺ ions and the
131 molecules R with a higher proton affinity than water (> 691 kJ mol⁻¹) (Hunter and Lias, 1998).



133 Thus, isomeric molecules (such as acetone and propanal) form the same product ion RH⁺ and cannot be distinguished.
134 For the purpose of investigating the atmospheric chemistry of carbonyl compounds, this is a major disadvantage since
135 the distribution between short-lived aldehydes and longer-lived ketones with the same carbon number remains unclear.
136 However, it has been shown that by using an alternative reagent ion (i.e., NO⁺), aldehydes and ketones can be

137 distinguished. NO⁺ ionizes aldehydes mainly via hydride abstraction (R2), whereas ketones and NO⁺ tend to form a
138 cluster (R3) leading to different product ions (Koss et al., 2016; Španěl et al., 1997).



141 To implement the NO⁺ chemical ionization mass spectrometer (NO⁺ CIMS), synthetic air instead of water vapor was
142 introduced in the ion source, and the source parameters were tuned to achieve a low contribution of impurity ions
143 (H₃O⁺, O₂⁺, NO₂⁺) and high counts of NO⁺. Two settings with varying E/N (electrical field strength to gas number
144 density) values were applied. One set had a relatively low E/N of 70 Td (Air (NO) = 9 sccm, U_{drift} = 500 V, p_{drift} =
145 3.4 mbar, T_{drift} = 60 deg C, U_{source} = 70 V), which has been recommended in previous studies to minimize
146 fragmentation (Koss et al., 2016; Romano and Hanna, 2018); the other was operated with 120 Td (Air (NO) = 9 sccm,
147 U_{drift} = 850 V, p_{drift} = 3.4 mbar, T_{drift} = 60 deg C, U_{source} = 70 V) for comparison. Low impurities of H₃O⁺ (≤ 1 %), O₂[±]
148 (< 0.01 %) and NO₂⁺ (< 2.5 %) were achieved using both settings.

149 The identity of the reaction that occurs to ionize the target compound depends on the thermodynamical properties of
150 the molecule. The hydride ion affinity of aldehydes is less than that of NO⁺, so R2 is exothermic and favored (Karl et
151 al., 2012; Španěl et al., 1997). Ketones do not show the same tendency to donate a hydrogen atom and the ionization
152 energies of most ketones, especially small ones, is slightly higher than that of NO (> 9.26 eV) (Smith et al., 2003).
153 Thus, an association reaction, R3, primarily occurs for the ketones in this study. Due to the humid conditions in the
154 rainforest, NO⁺(H₂O)-clusters were also available to react with ketones via ligand switching, producing the same
155 products as the association reaction R3 (Smith et al., 2003). The ionization energies of 3-hexanone, 2-heptanone, and
156 2-nonanone are smaller than or equal to that of NO; nevertheless, the association reaction has been shown to be favored
157 by selected ion flow tube (SIFT) studies (Španěl et al., 1997). Those compounds were, however, not detected in the
158 mass spectra obtained in the rainforest environment examined in this study.

159 Besides the most favored reaction, other ionization channels can also produce product ions. This, and partial
160 fragmentation in the drift tube can lead to additional complications of the mass spectra. To identify the distribution of
161 product ions and fragments of carbonyls for the type of instrument used in this study, a single-compound headspace
162 analysis was performed in the laboratory under humid conditions using a PTR-ToF-MS 8000. This is important as the
163 sensitivity of the carbonyl signals towards water originates from the formation of H₃O⁺ ions (and ionized water
164 clusters) that compete with NO⁺ and from the formation of NO⁺ water clusters. It should be noted that we accounted
165 for the humidity-dependent formation of (H₂O)NO⁺ by normalizing the signals to NO⁺ and (H₂O)NO⁺. The basic
166 components of the PTR-ToF-MS 8000 instrument, mainly the ion source, drift tube, and detector are similar to a PTR-
167 ToF-MS 4000, so that the relative transmission can be assumed to be identical. The instrument was tuned to have the
168 same E/N (electric field intensity divided by gas number density) in the drift tube and similar impurities (≤ 5 %) as
169 the instrument in the field. In both field and laboratory, two different settings for the E/N values were applied.
170 One set had a relatively low E/N of 70 Td, which has been recommended in previous studies to minimize
171 fragmentation (Koss et al., 2016; Romano and Hanna, 2018); the other was operated with 120 Td for comparison. The
172 results of the single-compound headspace analysis can be found in the Supplementary (Table S1).

173 The complexity of the mass spectra measured with a NO⁺ CIMS is a disadvantage if one aims for a non-targeted
174 analysis of VOC present in a certain environment, such as the rainforest. Long-term VOC observations at ATTO are
175 therefore conducted with a PTR-ToF-MS using H₃O⁺ ions. However, for a targeted analysis, specifically for separating
176 carbonyl compounds, the NO⁺ CIMS is a convenient method (Ernle et al., 2023; Karl et al., 2012; Koss et al., 2016).
177 Another advantage of the NO⁺ chemistry is the ability to detect certain alkanes, as their proton affinity is too low to
178 be detected by a PTR-MS (Koss et al., 2016). This has been widely used in urban or rural areas to quantify vehicle
179 emissions, but such species have not yet been investigated at the ATTO rainforest site (Chen et al., 2022; Wang et al.,
180 2020a).

181

182 2.3 VOC data analysis

183 Integration of the mass spectra, baseline-, and duty-cycle-correction were performed using the IDA software (Ionicon
184 Analytik). In a subsequent step, the obtained signals were normalized to NO^+ and $(\text{H}_2\text{O})_2\text{NO}^+$ and drift parameters like
185 pressure and temperature, to account for fluctuations.

186 Table 1 shows the sensitivities and limits of detection (LoD) for all target molecules with E/N values of 70 and 120 Td
187 applied. It was evident that the sensitivity of ketones decreases dramatically with high E/N conditions, most probably
188 due to enhanced fragmentation caused by more collisions in the drift tube.

189 Compounds displayed in bold in Table 1 were quantified using a primary VOC gas standard (Apel-Riemer
190 Environmental Inc., Colorado, USA). The calibration was performed using moisturized synthetic air mixed with the
191 VOC gas standard to mimic tropical conditions with 70 to 95 % relative humidity, typical for the ATTO site.
192 Unfortunately, this did not comprise all target carbonyls, and for those compounds not in the standard, a theoretical
193 method was applied to obtain concentrations, resulting in a higher uncertainty. The relative distribution of the product
194 ions obtained from the single-compound headspace analysis was used to correct for the fragmentation of carbonyl
195 compounds with higher m/z-ratios onto the parent m/z-ratios of other target compounds.

196 For those compounds not included in the gas standard, mixing ratios were obtained by calculating the ionization
197 efficiency with a previously determined reaction rate of NO^+ and the target compound under the current conditions in
198 the drift tube (k-rate analysis) (Cappellin et al., 2012).

$$199 \quad [\text{VOC}] = \frac{1}{c} \frac{[\text{VOC}^+]_{\text{ncps}}}{k t [\text{NO}^+]_{\text{ncps}}} \quad (1)$$

200 Here, k is the reaction rate, and t represents the reaction time in the drift tube, which can be approximated using the
201 length of the drift tube, the mobility of the primary ions and the applied drift voltage. Using Equation 1, the mixing
202 ratio of a VOC is calculated from the normalized measured signal (ncps = normalized counts per second) of the main
203 product ion. However, ~~T~~the reaction rates (k-rates), also presented in Table 1, have been experimentally derived for
204 the sum of all product ions. Thus, a weighting factor c for the relative production of the target ion ~~needed-needs~~ to be
205 applied, which was also obtained by the single-compound headspace analysis from the slope of the signals of the
206 target ion vs. other product ions. The mixing ratios of both E/N settings, obtained by applying Equation 1 with the
207 respective product ion distributions, agree well for most compounds (except for n-hexanal and ketones, which have a
208 low sensitivity at 120 Td). This accordance supports the assumption that product ion distributions were valid for both
209 instruments. To calculate propanal, the calibration factor of methacrolein was used, since in a previous calibration
210 measurement with the PTR-ToF-MS 8000 both compounds had similar sensitivities (methacrolein: 0.13 ppb ncps⁻¹,
211 propanal: 0.17 ppb ncps⁻¹).

212 The measurement uncertainty in the mixing ratios of standard calibrated VOC was less than 25%. It was derived from
213 the accuracy of the VOC gas standard ($\pm 5\%$), the flow meter used for the calibration ($\pm 1\%$), the accuracy of the least
214 square fit of the calibration curve (molecule-dependent, circa $\pm 10\%$), and the uncertainty of the relative distribution
215 of product ions, which was expected to be below 20%. The uncertainty of the product ion distribution was estimated
216 from the purity of the liquid carbonyls tested ($> 95\%$) as well as possible contamination during the headspace
217 sampling. In the case of theoretically calculated mixing ratios using k-rates the accuracy was accordingly higher. The
218 accuracy of the k-rate ($\pm 20\%$) (Španěl et al., 1997) and the accuracy of the distribution of product ions give the
219 absolute accuracy for k-rate calibrated mixing ratios which was thus estimated to be below 30%.

220 Detection limits were defined as three times the standard deviation of the background noise at the specified mass.
221 Those are also displayed in Figures 1–2. Negative values arising from the subtraction of the background were set to
222 zero to account for a slightly too high background measurement of some compounds during calibration.

223

224 2.4 Validation of observations

225 Pre-separation of the VOC with a GC column prior to detection with the NO^+ CIMS can indicate the pureness or
226 compound specificity of an m/z ratio. Koss et al., 2016 reported such data for urban ambient air and concluded that
227 certain masses can be seen as unambiguous in that environment. The E/N field used in that study, which strongly
228 impacts the fragmentation patterns on different m/z ratios, was similar to this study (60 Td), but the measurement site
229 was a parking lot in an urban area (Koss et al., 2016). Uncontaminated m/z ratios assigned to carbonyl compounds
230 were found for acetaldehyde, propanal, methacrolein, and crotonaldehyde, the sum of C_5 -aldehydes, acetone, hexanal,
231 MVK, methyl ethyl ketone (MEK), benzaldehyde, heptanal, the sum of C_5 -ketones, and octanal. Nevertheless,
232 biogenic compounds that may not be present in an urban environment were, therefore, not part of the GC method
233 applied in Koss et al. and remained as potential interferents for the carbonyl m/z ratios.

234 Allyl ethyl ether, an isomer of C_5 -carbonyls that also undergoes hydride transfer, was potentially such a candidate for
235 interfering in the C_5 -aldehyde m/z ratio (Smith et al., 2011; Španěl and Smith, 1998). The m/z ratio of C_5 -aldehydes
236 might have also been affected by 1-5 pentanediol if present at significant concentrations (Španěl et al., 2002). Some
237 carboxylic acids react with NO^+ under the drift tube conditions to form $\text{R} - \text{OH} + \text{HNO}_2$ and thus make isomers to the
238 ionized carbonyl species. Trimethylacetic acid was reported to mainly form $\text{C}_5\text{H}_9\text{O}^+$ and thus can also potentially
239 interfere with C_5 -aldehydes (Španěl and Smith, 1998).

240 N-butyric acid is part of the glucose metabolism in plants and, upon ionization, partly makes $\text{C}_4\text{H}_7\text{O}^+$ ions (m/z
241 71.0491); thus, it potentially interfered with butanal (Smith et al., 2011). The same holds for isobutyric acid. Also,
242 valeric acid has been shown to fragment into $\text{C}_4\text{H}_7\text{O}^+$ to a great extent (Španěl and Smith, 1998). For the alcohols 2-
243 butanol, 1,4-butanediol, and the ester methyl butyrate, fragmentation into $\text{C}_4\text{H}_7\text{O}^+$ has been shown to occur (Koss et
244 al., 2016; Španěl et al., 2002; Španěl and Smith, 1998). Tetrahydrofuran, an ether isomeric with butanal is ionized via
245 hydride transfer and also forms $\text{C}_4\text{H}_7\text{O}^+$ (Španěl and Smith, 1998). Contamination from 2-butanol was shown to
246 account for around 50% of $\text{C}_4\text{H}_7\text{O}^+$ at an urban site in Boulder, USA (Koss et al., 2016). Since 2-butanol has been
247 previously found in emissions from vegetation (Kesselmeier and Staudt, 1999) and the mixing ratios of $\text{C}_4\text{H}_7\text{O}^+$ were
248 close to the detection limit, butanal could not be investigated without potential bias from other oxygenated VOC. With
249 another measurement technique (sampling to adsorbent tubes and measurement with a GC-ToF-MS) applied at ATTO
250 also no significant butanal peak was found. However, butanal has been identified in the Amazonian atmosphere during
251 the dry and wet seasons at another site in 1999 (Andreae et al., 2002).

Table 1: List of identified carbonyl compounds and other hydrocarbons and their properties for detection with NO⁺ CIMS (PTR-ToF-MS 4000). Sensitivities are compared to the classical PTR-MS method using H₃O⁺ reagent ions. The “product factor” ζ represents the weighting factor for the k-rate obtained from the distribution of product ions as described in section 2.3. Compounds in bold were quantified using a primary standard.

Carbonyl species	Ion formula	Exact m/z	k-rate 10 ⁻⁹ cm ³ s ⁻¹	NO ⁺						H ₃ O ⁺
				E/N = 70 Td			E/N = 120 Td			E/N = 120 Td
				Prod. factor ζ	Sensitivity ppb ncps ⁻¹	LoD ppb	Prod. factor ζ	Sensitivity ppb ncps ⁻¹	LoD ppb	Sensitivity ppb ncps ⁻¹
Acetaldehyde	C ₂ H ₃ O ⁺	43.01784	0.6 (Španěl et al., 1997)	-	0.155	0.112	-	0.431	0.160	0.025
Acetone	C ₃ H ₆ NO ₂ ⁺	88.0393	1.2 (Španěl et al., 1997)	(0.43)	0.078	0.06	0.27	4.803	0.705	0.031
Propanal	C ₃ H ₅ O ⁺	57.0335	2.5 (Španěl et al., 1997)	(0.79)	0.046	0.053	0.82	0.256	0.049	-
MEK	C ₄ H ₈ NO ₂ ⁺	102.055	2.8 (Španěl et al., 1997)	(0.84)	0.049	0.008	0.61	1.027	0.111	0.028
MVK	C ₄ H ₆ NO ₂ ⁺	100.039	2.4 (Michel et al., 2005)	0.86	-	0.004	0.67	-	0.012	-
MACR	C ₄ H ₅ O ⁺	69.03349	2.6 (Michel et al., 2005)	(0.54)	0.046	0.021	0.42	0.256	0.093	0.028
n-pentanone	C ₅ H ₁₀ NO ₂ ⁺	116.0706	3.4 (Španěl et al., 1997)	0.85	-	0.005	0.56	-	0.007	-
n-pentanal	C ₅ H ₉ O ⁺	85.0648	3.2 (Španěl et al., 1997)	0.79	-	0.003	0.28	-	0.011	-
n-hexanone	C ₆ H ₁₂ NO ₂ ⁺	130.0863	3.3 (Španěl et al., 1997)	-	-	0.002	-	-	-	-
Hexanal	C ₆ H ₁₁ O ⁺	99.0804	2.5 (Španěl et al., 1997)	0.75	-	0.006	0.4	-	0.016	-
Trans-2-hexenal	C ₆ H ₉ O ⁺	97.0672	2.8 (Roberts et al., 2022)	0.68	-	0.006	0.82	-	0.005	-
Benzaldehyde	C ₇ H ₅ O ⁺	105.033	2.8 (Španěl et al., 1997)	0.96	-	0.005	0.97	-	0.003	-
Heptanal	C ₇ H ₁₃ O ⁺	113.0961	2	-	-	0.004	-	-	0.007	-
Octanal	C ₈ H ₁₅ O ⁺	127.1117	2.7 (Romano and Hanna, 2018)	0.81	-	0.004	0.61	-	0.004	-
Nonanal	C ₉ H ₁₇ O ⁺	141.1274	1.1 (Roberts et al., 2022)	0.04	-	0.145	0.1	-	0.078	-
Nopinone	C ₉ H ₁₄ O ⁺	138.1039	2	-	-	0.019	-	-	0.002	-
<i>Alkanes</i>										
Isopentane	C ₅ H ₁₁ ⁺	71.086	2	-	-	0.013	-	-	0.027	-
Methyl-cyclopentane	C ₆ H ₁₁ ⁺	83.086	2	-	-	0.005	-	-	0.008	-
2-, 3-methyl-pentane	C ₆ H ₁₃ ⁺	85.101	2	-	-	0.007	-	-	0.006	-
C ₇ cyclic alkanes	C ₇ H ₁₃ ⁺	97.101	2	-	-	0.004	-	-	0.003	-

Table 1 continued.

VOC species	Ion formula	Exact m/z	k-rate $10^{-9} \text{ cm}^3 \text{ s}^{-1}$	NO ⁺						H ₃ O ⁺
				E/N = 70 Td			E/N = 120 Td			E/N = 120 Td
				Pred. factor C	Sensitivity ppb ncps ⁻¹	LoD ppb	Pred. factor C	Sensitivity ppb ncps ⁻¹	LoD ppb	Sensitivity ppb ncps ⁻¹
C2-alkyl-cyclohexanes	C ₈ H ₁₅ ⁺	111.117	2	-	-	0.004	-	-	0.005	-
<i>Alkenes</i>										
C ₅ -alkene (2-pentenes)	C ₅ H ₁₀ ⁺	70.0777	2	-	-	-	-	-	0.009	-
C ₅ -alkene (α-olefin)	C ₅ H ₁₀ NO ⁺	100.076	2	-	-	0.006	-	-	0.003	-
C ₆ H ₁₀	C ₆ H ₁₀ ⁺	82.0777	2	-	-	0.006	-	-	0.01	
<i>Alcohols</i>										
Ethanol	C ₂ H ₅ O ⁺	45.0335	2	-	-	0.050	-	-	0.019	-
<i>Alkyne</i>										
Propyne	C ₄ H ₆ ⁺	54.046	2	-	-	0.026	-	-	0.011	-
<i>Aromatic</i>										
Benzene	C ₆ H ₆ ⁺	78.046	-	-	0.101	0.020	-	0.071	0.009	0.063
<i>Terpenes</i>										
Isoprene	C ₅ H ₈ ⁺	68.0621	-	-	0.078	0.018	-	0.068	0.023	0.045
Sum of mono-terpenes	C ₁₀ H ₁₆ ⁺	136.125	-	-	0.067	0.004	-	0.554	0.039	0.103
<i>Other</i>										
Furan	C ₄ H ₄ O ⁺	68.0258	2	-	-	0.008	-	-	-	-
C ₅ H ₄ O ₃	C ₅ H ₄ NO ₄ ⁺	142.014	2	-	-	0.005	-	-	0.003	-

253 Propionic acid is a potential contaminant for propanal on the m/z of C₃H₅O⁺, but only a fraction of the acid was found
 254 to land on the propanal m/z (Španěl and Smith, 1998). A higher fraction of the fragments of methyl and ethyl
 255 propionate were detected as isomers to ionized propanal but have not been found to be present in biogenic emissions
 256 so far (Kesselmeier and Staudt, 1999; Španěl and Smith, 1998).

257 It can also not be excluded that fragmentation to C₂H₃O⁺ of several species, in particular acetic acid, methyl formate,
 258 methyl acetate, and ethyl acetate contributes to the m/z ratio of acetaldehyde (C₂H₃O⁺). Experimental evidence for the
 259 contamination has only been found for a small contribution of methyl and ethyl acetate of less than 20% (Španěl and
 260 Smith, 1998).

261 The isomers hexanal and z-3-hexenol are known to be emitted together by damaged green leaves (Jardine et al., 2012a;
 262 Langford et al., 2010). A possible detection of both compounds on m/z of C₆H₁₁O⁺ could not be excluded, since
 263 alcohols also undergo hydride abstraction during the reaction with NO⁺ (Koss et al., 2016).

264 To our knowledge, none of the species that were demonstrated to fragment on the same m/z ratios as carbonyls have
 265 been reported to be abundant in forested environments or even to be biogenically emitted, except for z-3-hexenol, 2-
 266 butanol, n- and isobutyric acid, acetic acid, and propionic acid. In general, acids have primary sources, including
 267 biogenic emissions and biomass burning but also photochemical sources including the ozonolysis of alkenes
 268 (Orzechowska et al., 2005). The dataset from this study and comparison with the corresponding m/z of acids under

269 H₃O⁺ ionization that have been measured previously at the ATTO site suggested that carboxylic acids undergo an
270 association reaction with NO⁺. A headspace analysis with acetic acid also revealed no significant contributions to any
271 other m/z except the association product C₂H₄NO₃⁺.

272 Fragmentation from higher carbonyls to m/z ratios attributed to lower carbonyls was observed in the single compound
273 headspace analysis, conducted with aldehydes and ketones up to nonanal. The m/z of acetaldehyde (C₂H₃O⁺, 43.0178)
274 saw small contributions from acetone and pentanone, which were subtracted from the acetaldehyde signal. For this
275 correction, the relative contribution of the fragments from their parent mass, which was determined by the headspace
276 analysis, was used. A list of the single compounds and their product ions formed in the drift tube can be found in the
277 supplementary Table S1. Contributions from higher carbonyls in the NO⁺ CIMS were not likely since they were not
278 observed or were below the detection limit.

279

280 **3 Results**

281 **3.1 Atmospheric conditions and seasonality**

282 Seasonality in the central Amazon is characterized by a comparatively less polluted wet season (February–May) and
283 a more strongly polluted dry season, due to the more frequent influence of biomass burning (August–November)
284 (Holanda et al., 2023; Pöhlker et al., 2019). The NO⁺ CIMS measurements took place from June 23 until July 8 and
285 from September 27 until October 14, 2019. Below, we outline the meteorological conditions during both measurement
286 periods as they influenced seasonal variations in observed VOC mixing ratios and correlations. It is important to
287 consider that the photochemical loss of VOC and reactions involving OH depend on the availability of sunlight, which
288 also affects the secondary formation of OVOC from the oxidation of different hydrocarbons. VOC emissions from
289 vegetation are driven by light (photosynthetically active radiation, PAR), temperature, water availability, air pollution,
290 and biotic factors, such as herbivore infestation, pathogenic infections, or the developmental stage of a plant
291 (Laothawornkitkul et al., 2009). However, at heights above 80 m, integrated VOC emissions from a whole forested
292 area domiciled by various plant and herbivorous species at all developmental stages were sampled. As has been
293 reported previously, inter-seasonal growth variations may even induce the plant to switch from isoprene emission to
294 monoterpene emission and back (Kuhn et al., 2004a, b). The growth of new leaves (leaf flush), which are
295 photosynthetically more effective than mature leaves peaks in the dry season and is correlated with the availability of
296 light (Restrepo-Coupe et al., 2013), which causes an inter-seasonal gradient possibly manifested in the presented
297 BVOC emissions. The emission and uptake of BVOC by soils and cryptogamic organisms was shown to depend on
298 the availability of water and could additionally contribute to observed seasonal differences in BVOC concentrations
299 (Bourtsoukidis et al., 2018; Edtbauer et al., 2021).

300 On average, daytime temperatures differed by only 0.4 °C between the transition (June – July) and the dry season
301 (Fig. S3). Maximum temperatures in the canopy (at 26 m) were reached at 12:00 local time (LT), with 30.5 °C in the
302 transition season and 31.2 °C in the dry season on average. The diurnal evolution of temperature closely followed the
303 incoming solar radiation, here represented by PAR. Dry season observations of PAR were higher by about 9%
304 compared to the transition season. Precipitation in the month before the NO⁺ CIMS measurements took place totaled
305 157 mm in June and 119 in September 2019 (Fig. S4). The water level measured in the Rio Negro close to Manaus in
306 2019, however, exhibited maximum values in June and minimum values in October, with a difference of about 10 m
307 (Chevuturi et al., 2022).

308 The sampled air originated predominantly from the east (SE to NE); thus, an influence from the city of Manaus could
309 be excluded (Fig. S1). However, for long-lived anthropogenic alkanes, influence from populated areas along the
310 Amazonas and smaller side rivers was conceivable. The detected alkanes (Table 1) had low mixing ratios below the
311 detection limit, indicating no significant influence from industries based on fossil fuel combustion.

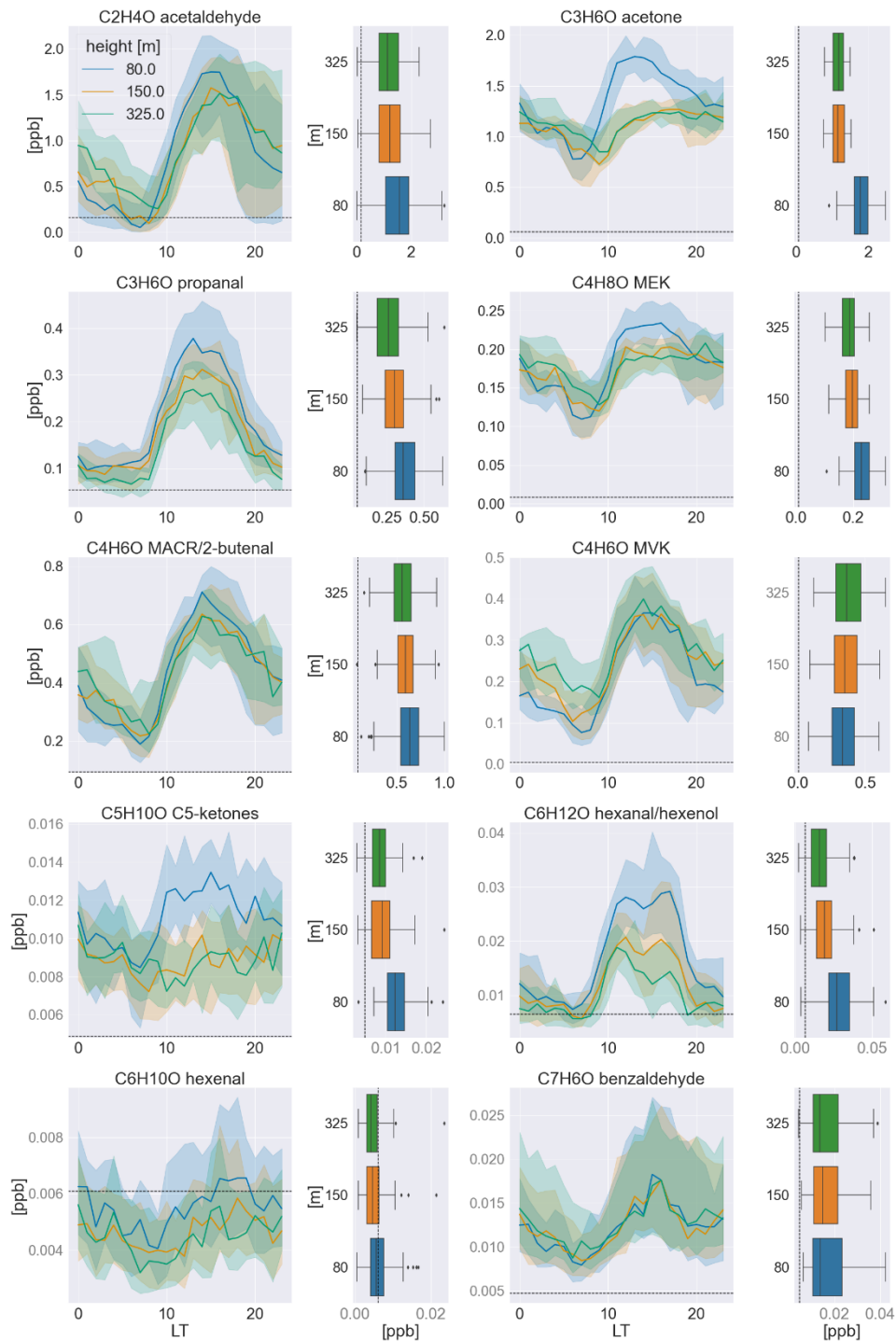
312 Black carbon (BC) was used as a marker of biomass burning emissions. BC sampled at ATTO has been shown to
313 originate from biomass burning in South America and Africa (Holanda et al., 2020, 2023). Enhanced concentrations
314 of 0.42 and 0.54 µg m⁻³ (80, 325 m) were found on average in the 2019 dry season. Maximum concentrations reached

315 0.93 and 1.17 $\mu\text{g m}^{-3}$. Average concentrations of 0.18 and 0.21 BC (80, 325 m) in the transition season indicated less
316 polluted conditions. A large number of VOC, including certain carbonyl compounds, are usually co-emitted during
317 biomass burning with various emission factors and rates (Andreae, 2019; Andreae and Merlet, 2001). Therefore, the
318 carbonyls detected with the NO^+ CIMS during this study and their precursors potentially originated from both biogenic
319 and biomass burning sources. Correlations of carbonyls with BC at 325 m are shown in the Supplementary Data for
320 both seasons (Fig. S5) to detect possible influences from advected, fresh, or aged biomass burning plumes. In the cases
321 of acetaldehyde, acetone, methacrolein, MVK, and benzaldehyde, a Pearson coefficient of $p > 0.55$ was calculated for
322 the day and nighttime so that an influence of biomass burning through co-advection or in plume production was
323 feasible.

324

325 **3.2 Vertical distribution of carbonyls above the canopy**

326 The distribution of carbonyls with height above the uniform rainforest-covered landscape provides information on the
327 nature of emission sources, oxidative transformations, and carbonyl sinks under consideration of dynamic processes
328 in the atmospheric mixed layer. Vertical gradients were governed by the strength and temporal variance of the
329 respective source and of surface uptake, the atmospheric lifetime of the species considered, and dilution through
330 turbulent mixing or entrainment from the free troposphere during mixed layer growth. Earlier work investigated the
331 chemical and dilutive loss of isoprene with height using observations at ATTO and a turbulence-resolving large eddy
332 simulation (DALES). It was shown that slightly more than 50% of the isoprene loss in the vertical (80–325 m) at noon
333 occurred due to dilutive turbulent mixing (Ringsdorf et al., 2023). It is important to note that the lowest sampling
334 height at 80 m was within the roughness sublayer. This is a layer within the mixed ABL of about 2–3 times the canopy
335 height (≈ 35 m), which is strongly affected by the tall canopy with respect to wind fields and, thus, turbulence. Within
336 this layer, the exchange between the canopy and atmosphere occurs by inhomogeneous flows into and out of the
337 canopy (Chamecki et al., 2020). An important process influencing the ambient concentration of the compounds
338 presented at all sampling heights was the growth of the ABL (up to 2 km height) after sunrise due to the strengthening
339 of turbulences from thermal expansion of the heated air masses near the ground. During ABL growth, air from higher
340 altitudes (residual



341

Figure 1: Median averaged timeseries in the wet-to-dry transition season (June/July) of 2019 measured at all sampling heights for each carbonyl compound and its respective vertical profile at noon (12:00–15:00 LT) to the right. The shadings indicate the quartiles (25th and 75th). In the box-and-whisker plots, the boxes also represent the quartiles, while the residual data except for outliers are included in the whiskers. The detection limit (3 sigma) is indicated by dashed, black lines. The mixing ratios in black font were calibrated to a standard, while those in grey font were calculated based on the k-rate.

342

343 layer containing more chemically aged air) is entrained, leading to the minimum mixing ratios observed after 06:00 LT
344 at all three heights. During the day, turbulent mixing via convection and associated downward motions is strongest
345 until convection eases with decreasing insolation. At night, a stable stratification associated with low vertical mixing
346 is formed (Jordi Vilà-Guerau de Arellano, et al., 2015).

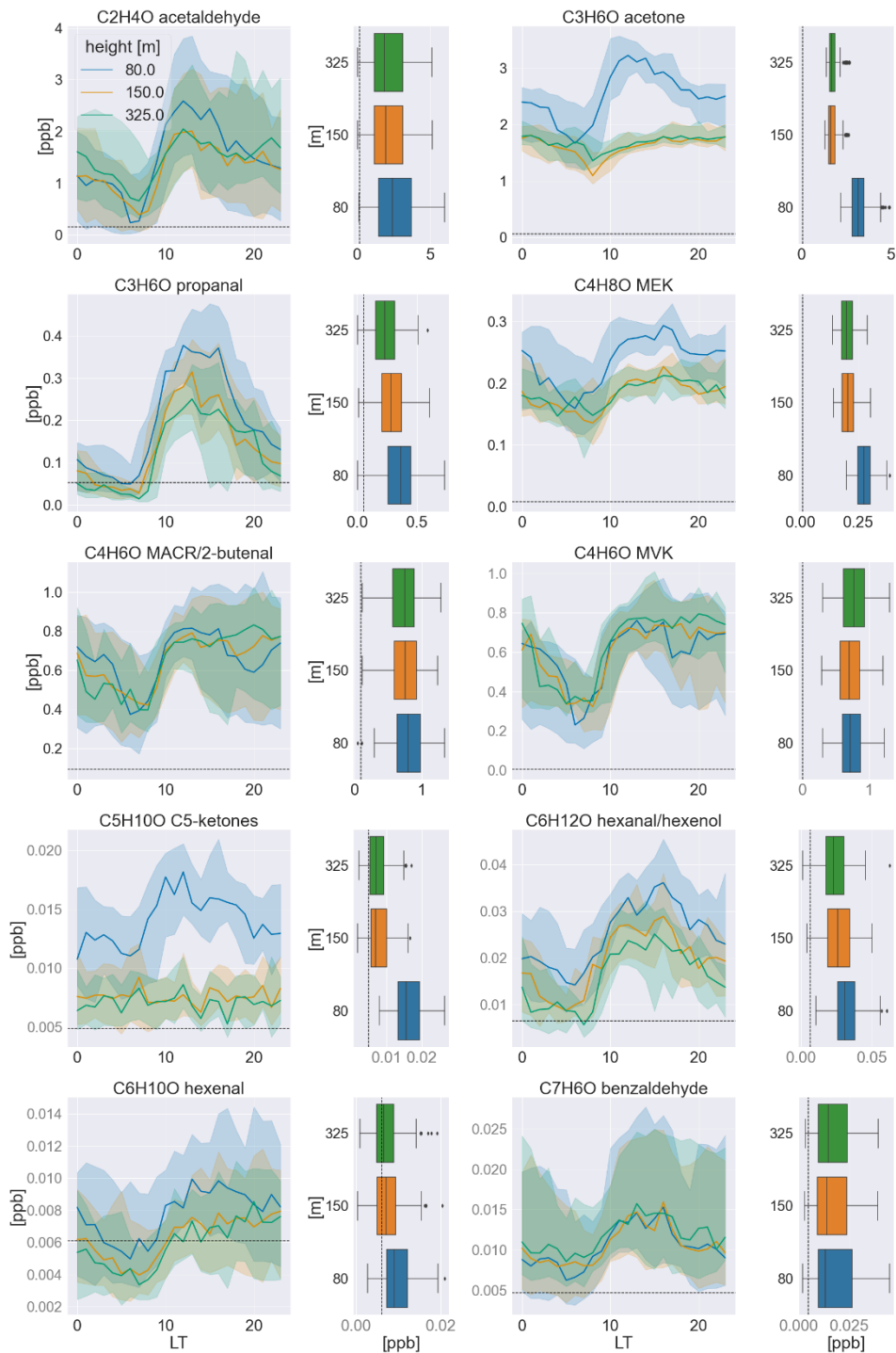
347 Under the reasonable assumption of a carbonyl source at canopy level (based on emission inventories discussed in
348 [Chapter-section 4](#)), the long-lived ketones were expected to have a background concentration in the convective mixing
349 layer but also above, while levels of short-lived aldehydes will tend to be zero at higher altitudes, ~~like-analogous to~~
350 isoprene. Consequently, the aldehydes should show a stronger decrease in their vertical profiles than the ketones,
351 which were expected to be well-mixed at about a hundred meters above the canopy throughout the convective mixing
352 layer. Nonetheless, one has to also take the secondary chemical formation of carbonyls into account, which can
353 influence the vertical gradients depending on the emission source and atmospheric lifetime of the precursors.

354 Figures 1 and 2 present the diurnal cycle observed at the three sampling heights for all carbonyls measured in the wet-
355 to-dry transition and the dry season, respectively. Some compounds were measured in very low concentrations, below
356 the detection limit in one or both seasons, namely, the sum of C₅-aldehydes, C₆-ketones, heptanal, octanal, and
357 nonanal. All other carbonyls showed distinct diurnal variabilities with increasing concentrations after sunrise
358 (06:00 LT) and decreasing concentrations at nighttime. Their diurnal cycle followed the evolution of PAR and
359 temperature with a slight delay throughout the day, reflecting the expected biogenic emission and photochemical
360 production. [Time series of the aldehydes and ketones are provided in the supplementary \(Fig. S6-S15\)](#). As
361 hypothesized above, no significant vertical variability was found for ketones, though only at 150 and 325 m, whereas
362 a strong decrease in mixing ratio with height was observed between 80 and 150 m. This distribution indicates that
363 mixing ratios of ketones were only well-mixed above 150 m, while the measurements at 80 m were influenced by a
364 strong source of ketones, which is discussed compound-wise below. The observed aldehydes exhibited different
365 vertical distributions; some showed increasing mixing ratios with height, others were rather steadily decreasing as it
366 was hypothesized, and some showed very small variabilities throughout the lowermost 325 m of the atmosphere.

367

368 **3.3 Correlations at 80m and common sources**

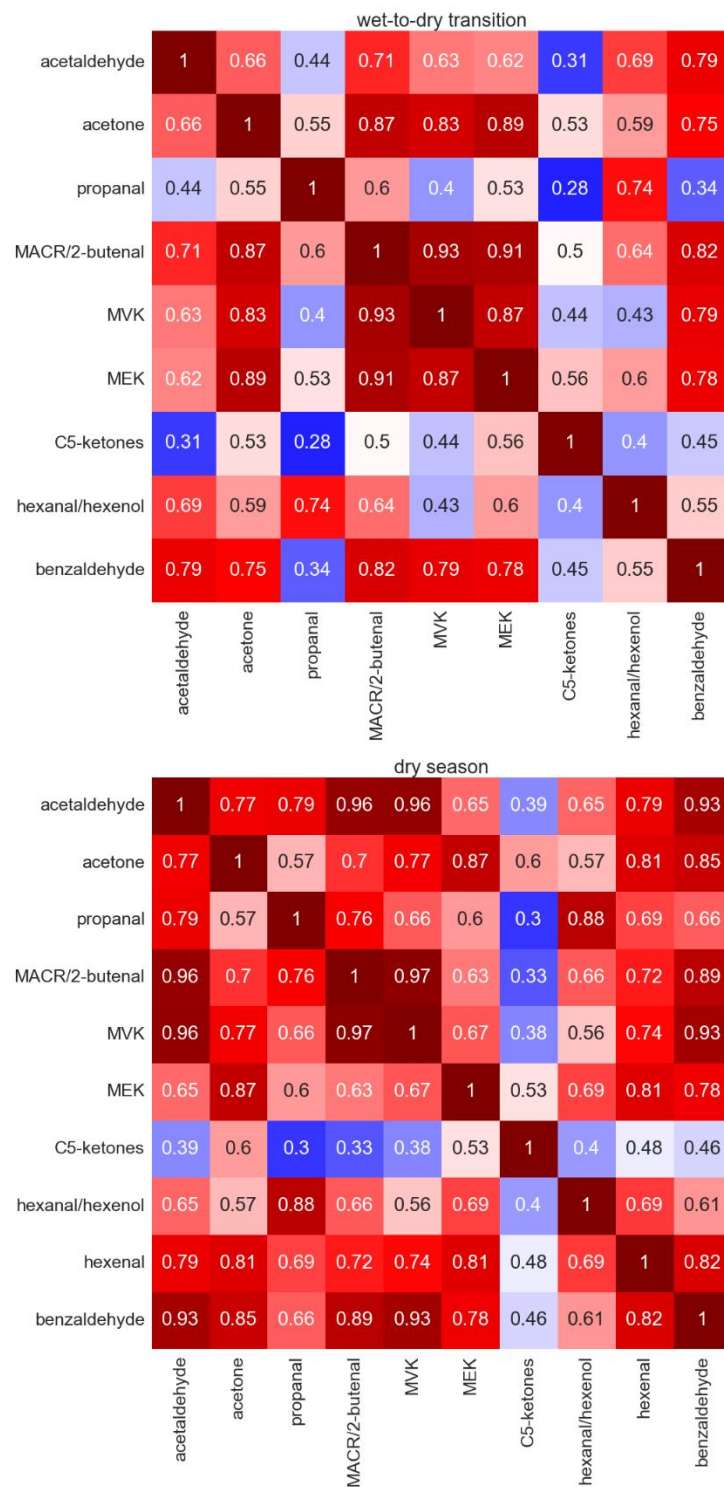
369 The chemical composition of airmasses measured at 80 m was governed by various processes occurring from the leaf
370 level up to mixing scales of the lower atmosphere. At the leaf level, BVOC are formed by plant metabolic pathways
371 or, possibly, in the case of OVOC, including carbonyls via within-leaf reactions. Epicuticular waxes, also called leaf
372 waxes, consist of long-chained hydrocarbons, e.g., the triterpene squalene, which yield OVOC during ozonolysis.
373 Depending on the position of the double bond of the long-chained molecule and its functional groups, aldehydes or
374 ketones are formed, whereby the chances for the formation of short-chained carbonyls like acetone are highest
375 (Fruekilde et al., 1998). Following their emission, a fraction is deposited on surfaces, which is in most cases reversible,
376 or taken up by stomata, which represents a potential sink (Niinemets et al., 2014). Depending on their atmospheric
377 lifetime, BVOC undergo within-canopy oxidation; in the case of reactive isoprene and monoterpenes, this was found
378 to come to not more than 10% of their initial emission flux (Fuentes et al., 2022; Karl et al., 2004) before being ejected
379 from the canopy. Within and above the canopy they are mixed



380

381

Figure 2: Median averaged timeseries in the dry season (September/October) of 2019 measured at all sampling heights for each carbonyl compound and its respective vertical profile at noon (12:00–15:00 LT) to the right. The shadings indicate the quartiles (25th and 75th). In the box-and-whisker plots, the boxes also represent the quartiles, while the residual data except for outliers are included in the whiskers. The detection limit (3 sigma) is indicated by dashed, black lines. The mixing ratios in black font were calibrated to a standard, while those in gray font were calculated based on the k-rate.



382

Figure 3: Pearson correlation coefficients for the intercorrelation of carbonyl species in the wet-to-dry transition season (upper) and in the dry season (lower).

383 air masses of varying ages and secondary production and depletion take place simultaneously. When correlating two
 384 time series of BVOC measured at that height, a high correlation coefficient can indicate similar production and loss

385 or possibly a precursor–product relationship. Here, it is very important to consider the timescales of production and
386 loss versus vertical transport since the residence time of airmasses in the first 80 m is limited during daytime
387 convective conditions. In a previous study, the mixing timescale, which accounted for turbulent up and downward
388 motions between 80 and 325 m at ATTO, was determined to range on average from 60 minutes at 10:00 LT to 15 min
389 at 15:00 LT (Ringsdorf et al., 2023). Based on that study, we assumed the mean residence time between the canopy
390 and 80 m to be in the same time range of minutes to 1 hour. Carbonyl precursors including alkenes, isoprene, higher
391 terpenes, and alkanes have atmospheric lifetimes with respect to oxidation by OH radicals of $\tau > 2$ hours, $\tau \approx 3$ hours,
392 minutes to hours, and days to weeks for the much less reactive alkanes (Altshuller, 1991; Wolfe et al., 2011). The
393 lifetimes with respect to OH of carbonyl compounds themselves range from 12 hours (trans-3-hexenal) (Jiménez et
394 al., 2007) to 119 days (acetone) and are even shorter when considering photolysis, which is a significant sink for
395 carbonyls (Mellouki et al., 2015). In Table 2, the lifetimes of carbonyls with respect to an average OH concentration
396 of 1×10^6 molecules cm^{-3} based on a previous study at the ATTO site are presented. This is the average over roughly
397 the same time of day that was considered for carbonyl correlations (10:00–15:00) (Ringsdorf et al., 2023). However,
398 isoprene oxidation was observed by the daily increase of the product MVK between 80 and 325 m.

399 Thus, correlations at 80 m will reflect only the processes that occur on a comparable or faster timescale than mixing.
400 This includes primary emissions, product formation in the atmosphere from short-lived precursors like alkenes and
401 terpenes, and progressive photochemical degradation/photolysis of short-lived carbonyls as well as loss via deposition.

402 Figures 3-4 show the Pearson correlation coefficients (ρ) for both seasons divided into day (10:00–17:00 LT) and
403 nighttime (22:00–05:00 LT) between the carbonyl compounds and between carbonyls and other selected VOC,
404 including terpenes (isoprene, sum of monoterpenes), alkenes (C_5 -alkenes, benzene), and oxygenated compounds
405 (ethanol, furan, acetic acid, $\text{C}_5\text{H}_4\text{O}_3$), when measured above the detection limit. Their diel and vertical distributions
406 are presented in the supplementary figures S16–S17. $\text{C}_5\text{H}_4\text{O}_3$ is a highly oxygenated compound, which was classified
407 to be exclusively an oxidation product of very reactive BVOC in a previous study conducted within and above a pine
408 forest. Therein, emission rates of very reactive BVOC were estimated to reach 6–30 times the emission rates of
409 monoterpenes (Holzinger et al., 2005). In this study, the highest mixing ratios were found at 325 m, suggesting that
410 besides being formed as a first-order oxidation product close to the canopy it was also a higher-order oxidation product
411 that therefore emerges at longer timescales. Very reactive BVOC presumably also represent precursors for carbonyl
412 compounds. Periods with precipitation were excluded from the correlations to avoid the effects of downbursts and
413 washout. As expected, high correlations were found between isoprene and the sum of monoterpenes, which are all
414 primary emissions that depend strongly on light and temperature. Correlation of carbonyl compounds with isoprene
415 and monoterpenes was preferred over PAR and temperature to identify light- and temperature-dependent direct
416 emission, due to the temporal delay between emission and detection. However, it is striking that most carbonyls

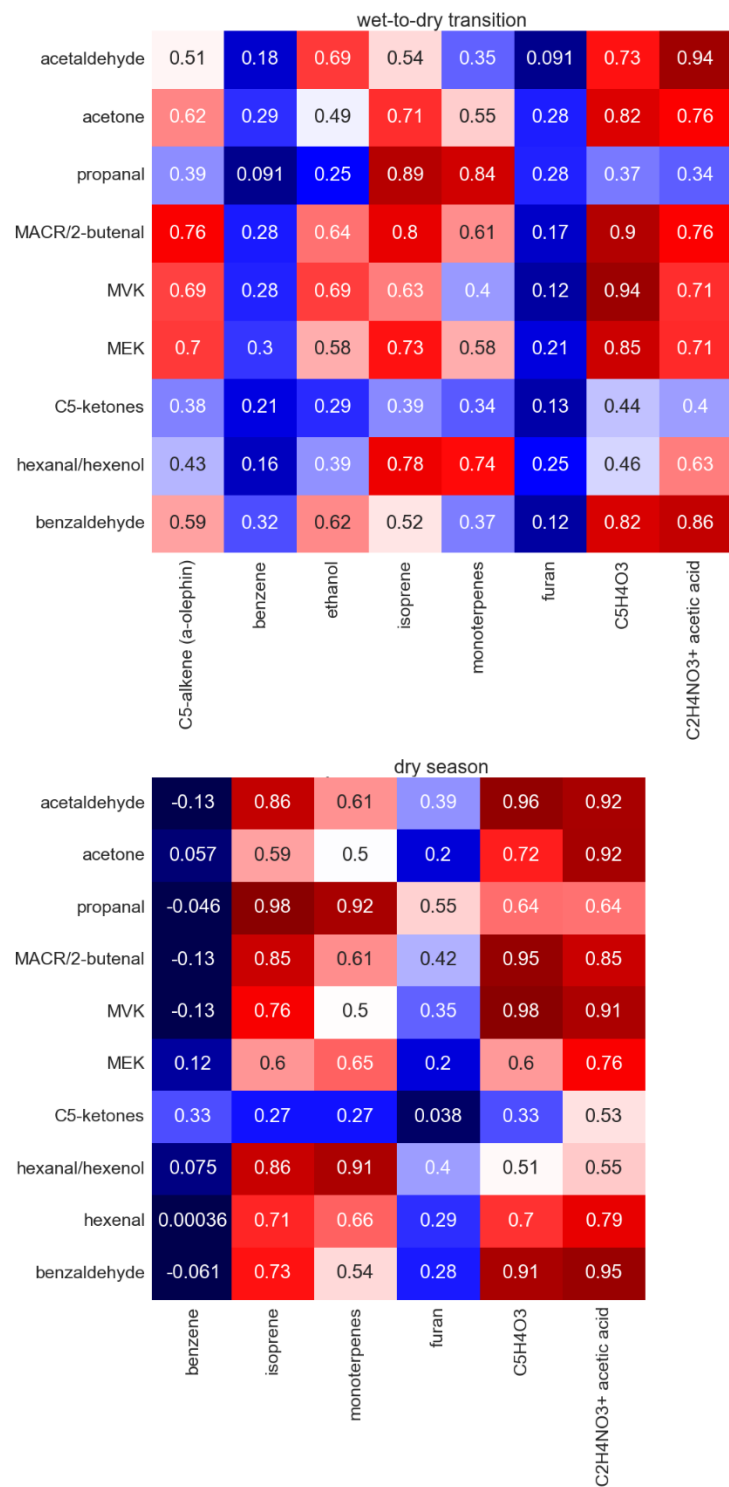
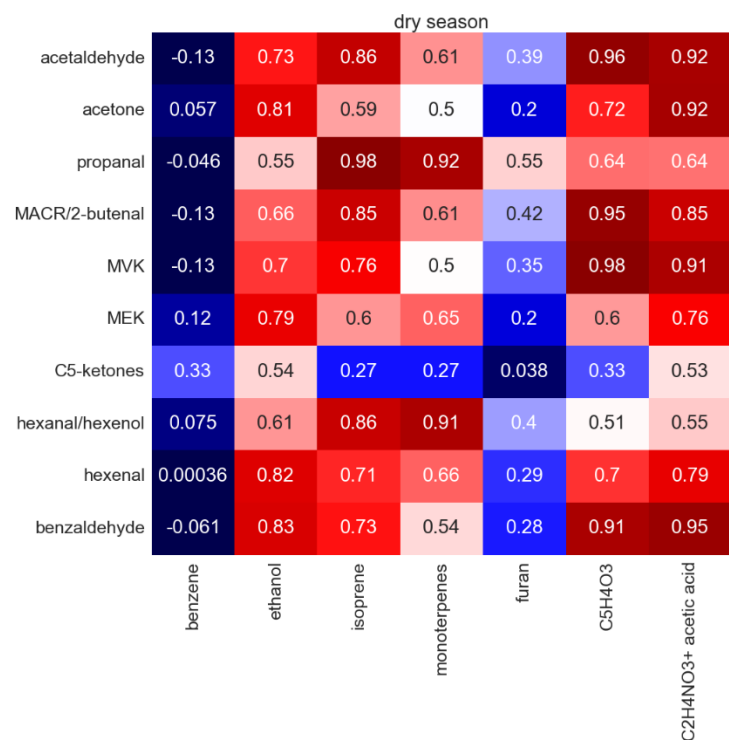
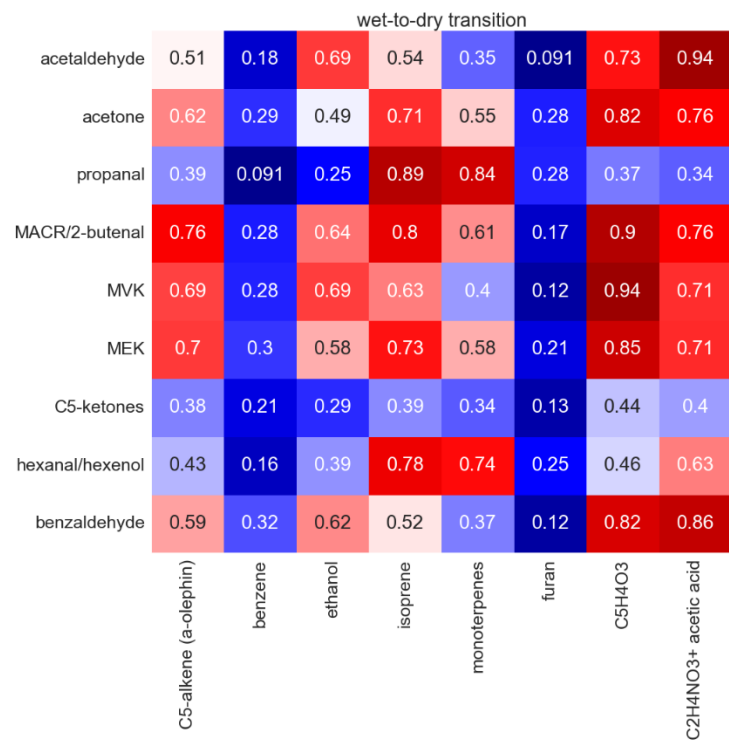


Figure 4: Pearson correlation coefficients for the correlation of carbonyl species with selected hydrocarbons in the wet-to-dry transition season (upper) and the dry season (lower).

417 showed significant correlations with all other carbonyls with Pearson coefficients greater than 0.7. This likely resulted
 418 from the common driving variables, namely light and temperature for emission, as well as similar photochemical



419 production rates.

420 The highest correlations with the primary emitted isoprene and monoterpenes were obtained for propanal and n-
 421 hexanal. Other compounds that were found to correlate very well were acetaldehyde, methacrolein, MVK, and C₅H₄O₃
 422 as well as acetone and MEK.

423 **3.4 Nocturnal loss rates**

424 Biogenic emissions unrelated to photosynthesis might have continued during the night, whereas oxidative chemistry
425 and, thus, secondary production of carbonyls was limited to reactions with O₃ and NO₃, which were found at low
426 levels in the remote forested atmosphere. Important loss mechanisms at night are deposition to surfaces and reaction
427 with NO₃ (Brown and Stutz, 2012). Deposition at night is thought to happen via adsorption to the cuticle of the leaves,
428 since stomata are closed in the absence of light. However, there is evidence that the stomatal conductance is maintained
429 at night by many woody species, implying an irreversible uptake for BVOCs that can be further processed and
430 converted to other metabolites (Niinemets et al., 2014). Reaction with NO₃ at nighttime is limited to unsaturated
431 BVOC but is also efficient for some saturated aldehydes. Assuming a rather high mixing ratio of 10 ppt NO₃ (Brown
432 and Stutz, 2012; Khan et al., 2015), nighttime atmospheric lifetimes of 8 days are estimated for n-hexanal, the most
433 reactive observed aldehyde with respect to NO₃. Ozone is circa 1000 times more abundant than NO₃, but the reaction
434 rates with carbonyls are much lower. Therefore, deposition is expected to be the dominant loss mechanism for
435 carbonyls at night. Table 2 summarizes properties of the observed carbonyl compounds that are important driving
436 variables of deposition on surfaces together with their observed loss rates during the night. These rates were obtained
437 by linear regression of the observed nocturnal time series at 80 m between 22:00 and 04:00 LT. Since the uptake of
438 BVOC by leaves occurs only when the ambient concentration exceeds the concentration in the inter-leaf space, high
439 loss rates were observed for BVOC with high ambient mixing ratios. However, the concentration gradient can be
440 maintained by a metabolic transformation of the BVOC in the leaf. Table 2 also includes the reactivity of BVOC
441 towards the OH radical, O₃, and NO₃.

442

443 **4 Discussion**

444 In the following sections, the diel variability, vertical distribution (80–325 m), and correlations between all measured
445 BVOC are considered in a compound-wise manner. The measurements presented here are related to previous studies
446 on the emission, formation, and loss of the carbonyl species.

447 **4.1 Acetaldehyde**

448 Acetaldehyde (ethanal) is known to be an important contributor to the total ambient carbonyl concentration in the
449 atmosphere. Various sources of acetaldehyde have been characterized previously, including direct emissions from
450 vegetation and the ocean and secondary production from the OH-, NO₃-, and O₃-initiated photooxidation of
451 hydrocarbons (Rottenberger et al., 2004; Wang et al., 2020b). Direct biogenic emissions may be of special importance
452 for the Amazonian rainforest, as acetaldehyde and ethanol release have been reported to result from root anoxia
453 (Bracho-Nunez et al., 2012; Holzinger et al., 2000; Rottenberger et al., 2008). This may occur in large areas caused

Table 2: Rate coefficients for the reaction with OH, NO₃, and O₃ and the atmospheric lifetime considering an OH radical concentration of 1x10⁶ molecules cm⁻¹. The rate coefficients and boiling point temperature were taken from the NIST database. Water solubility has been reported by Sander et al., 2023. The loss rate is calculated based on the median averaged slopes of the nocturnal (22:00–04:00) carbonyl timeseries.

VOC species	k _{OH} [cm ³ # ⁻¹ s ⁻¹]	Estimated lifetime Amazon [days]	k _{NO₃} [cm ³ # ⁻¹ s ⁻¹]	k _{O₃} [cm ³ # ⁻¹ s ⁻¹]	Volatility (T _{boil} [K])	Water- solubility (H _s ^{CP}) [mol m ⁻³ Pa ⁻¹]	Loss rate [ppb min ⁻¹] (transition, dry season)
Acetaldehyde	1.6E-11	1.4	2.4E-15	3.4E-20	294	1.3E-1	-6.7E-4, -1E-3
Acetone	1.9E-13	119.3	8.5E-18	8.5E-18	329	2.7E-1	-7.8E-4, -9.5E-4
Propanal	2E-11	1.2	6.2E-15	-	322	9.9E-2	-8.9E-5, -1.4E-4
MEK	1.2E-12	19.3	-	2.06E-16	353	1.8E-1	-8.4E-5, -7.4E-5
MVK	1.9E-11	1.25	1.2E-16	4.48E-18	354	4.0E-1	-1.1E-4, -4.8E-4
MACR	3E-11	0.75	3.3E-15	1.09E-18	341	4.5E-2	-2.1E-4,
2-Butenal	3.6E-11	0.64	5.1E-15	1.58E-18	375.5	5.9E-1	-2.1E-4
2-pentanone (C ₅ -ketones)	4.6E-12	5.08	-	-	375	1.3E-1	-
n-hexanal	2.8E-11	0.83	1.1E-14	-	402	4.5E-2	-2E-6
Z-3-hexenol	1E-10	0.21	2.7E-13	6.4E-17	427.7	-	-
z-2-hexenal	4.4E-11	0.52	1.2E-14	2.0E-18	419.7	1.4E-1	-
Benzaldehyde	1.3E-11	1.78	2.01E-15	2.0E-19	452	4.0E-1	-7.9E-6, -8E-6
Isoprene	1E-10	0.23	6.7E-13	1.28E-17	307	1.3E-4	-1.5E-3, -2.6E-3
α-pinene	5.3E-11	0.43	6.2E-12	9.6E-17	430	7E-4	1.7E-4, -3.2E-4

454 by seasonal flooding (Parolin et al., 2004). At 80, 150, and 325 m in the wet-to-dry transition season of 2019, observed
455 mean diurnal concentrations were 642, 702, 852 ppt, respectively, and 1.38, 1.25, 1.47 ppb in the dry season of 2019.

456 Metabolic production pathways of acetaldehyde within plants and subsequent emission have been found to occur not
457 only during root-flooding but also during rapid light-dark transitions (Fall, 2003; Holzinger et al., 2000). The anaerobic
458 conditions at the root's surface during flooding cause the ethanolic fermentation pathway to form ethanol that is
459 transported to the leaves of the plant to provide an energy source.

460 Acetaldehyde is an intermediate of this pathway which tends to leak out to the atmosphere due to its high volatility
461 (Kreuzwieser et al., 2000). Some Amazonian tree species can switch to fermentative metabolism (Bracho-Nunez et
462 al., 2012), but concentration or flux measurements during the dry-to-wet transition in Amazonia under field
463 conditions are missing. In this study, a strong correlation was found for ethanol and acetaldehyde in the nighttime
464 during the transition season (p = 0.92). The high correlation coefficient at 80 m could originate from similar sinks,
465 such as deposition to the canopy or related sources, such as the ethanolic fermentation pathway. Ethanol mixing ratios
466 were ten times higher in the transition season and showed a diel maximum at nighttime. Since river levels were at
467 their maximum levels in the transition season, root flooding may be partially responsible for the seasonal variability

Table 3: Median averaged mixing ratios of the observed carbonyl compounds for the measurement periods in the dry-to-wet transition and the 2019 dry season. The range presents the lowest mixing ratio included in the 25th and the highest mixing ratio included in the 75th quantile of the median averaged diurnal cycle. Numbers in italics represent the limit of detection.

Carbonyl species	Height [m]	Wet-to-dry transition – Jun-Jul 2019		Dry season 2019 – Sep-Oct 2019	
		Median [ppt]	Range [ppt]	Median [ppt]	Range [ppt]
Acetaldehyde	80	642	24 - 2043	1380	<i>160</i> - 3179
	150	702	24 - 1801	1252	239 - 3134
	325	852	59 - 1883	1472	256 - 3716
Acetone	80	1333	559 - 2083	2546	1155 - 3812
	150	1124	494 - 1509	1657	918 - 2105
	325	1146	661 - 1545	1707	1087 - 2115
Propanal	80	176	71 - 438	165	<i>53</i> - 410
	150	150	58 - 365	115	<i>53</i> - 349
	325	119	<i>53</i> - 348	85	<i>53</i> - 305
MEK	80	177	82 - 267	249	116 - 348
	150	175	81 - 229	188	98 - 259
	325	177	105 - 240	185	75 - 247
MVK	80	184	45 - 483	607	100 - 994
	150	229	53 - 481	599	164 - 967
	325	265	93 - 499	659	239 - 1014
MACR/2-Butenal	80	415	149 - 755	679	250 - 1026
	150	425	149 - 697	644	307 - 1010
	325	439	181 - 694	644	281 - 996
C ₅ -ketones	80	11	7 - 18	14	7 - 23
	150	9	7 - 15	8	7 - 13
	325	9	7 - 15	7	7 - 12
n-hexanal/ hexenols	80	15	6 - 50	26	6 - 53
	150	11	6 - 33	19	6 - 42
	325	9	6 - 30	16	6 - 43
z-2-hexenal	80	-	< 11	8	6 - 14
	150	-	< 9	-	< 12
	325	-	< 9	-	< 12
Benzaldehyde	80	12	6 - 27	11	6 - 26
	150	12	6 - 24	10	6 - 26
	325	12	6 - 24	11	6 - 25

468 of ethanol (Kirstine and Galbally, 2012). However, acetaldehyde showed a different seasonal variability, indicating
469 that other sources than those of ethanol were dominant. It is important to keep in mind that the ATTO site is a “Terra
470 firme” region with inundation events rare. Field measurements of roots under anoxia are still missing. Fast light–dark
471 transitions occur continuously inside the forest canopy and are suspected to lead to an overproduction of cytosolic
472 pyruvic acid in the leaves that is converted to acetaldehyde as a safety mechanism against acidification (Fall, 2003).
473 The wounding of a plant through cutting or drying out of plant tissues also leads to release of acetaldehyde (Guenther,
474 2000). The compound is also found in emissions from leaf litter presumably as a byproduct of biomass degradation
475 (Karl et al., 2003; Schade and Goldstein, 2001). Furthermore, the oxidation of polyunsaturated fatty acids in leaves
476 leads to the formation of reactive aldehydes, which can represent a primary source for many aldehydes, including
477 acetaldehyde (Matsui et al., 2010; Niinemets et al., 2014). Once released, the atmospheric lifetime of acetaldehyde is
478 in the range of 1.4 days with respect to OH (Table 2).

479 Tree branch enclosures and vertical gradient measurements at another Amazonian measurement site (Rondônia) in
480 1999 revealed that the canopy's role as a sink can even exceed its function in emissions. Uptake to leaves mainly
481 occurred via the leaf stomata and has been reported to be governed by a compensation point that varies between
482 canopy and understory species. The authors concluded that the observed ambient concentrations were generated
483 mainly by the secondary photochemical production of acetaldehyde (Rottenberger et al., 2004). Accordingly, in 2013,
484 measurements of acetaldehyde using a PTR-quadrupole-MS (nominal m/z 45) vertical gradients below 80 m at ATTO
485 showed increasing acetaldehyde between 24 m (inside the canopy, high influence by surrounding trees) and 79 m.
486 However, interestingly, this has only been observed in the dry season (Sep), whereas during the wet season of 2013
487 (Feb/Mar), a dominance of primary emission over secondary production was indicated by decreasing concentrations
488 directly above the canopy (Yáñez-Serrano et al., 2015). We observed decreasing mixing ratios at altitudes above 80 m
489 under dry season or close to dry season conditions in 2019. At noon, the acetaldehyde mixing ratios peaked in the first
490 150 m above the canopy, consistent with a rapid secondary production and a possible contribution from direct
491 emission. Primary emission might vary in strength and dominance with season due to the variability of light,
492 temperature, precipitation, and soil moisture and due to plant phenology. At 150 and 325 m, similar mixing ratios
493 were measured, suggesting well-mixed conditions and ongoing secondary formation between those heights, due to the
494 many routes of acetaldehyde photochemical generation.

495 In the rainforest environment, sources of the photochemical precursor hydrocarbons of acetaldehyde are most likely
496 to be natural emissions or longer-lived emissions from distant biomass burning. Aldehydes are a common product of
497 any hydrocarbons that are oxidized in the atmosphere (Calogirou et al., 1999; Mellouki et al., 2015). Laboratory
498 experiments showed that acetaldehyde emerges from the oxidation of alkanes and alkenes, with ethane and propene
499 having the largest emission fluxes globally (Singh et al., 2004). Ethane is globally distributed; thus, background
500 concentrations of acetaldehyde are generated by this route, which are, however, low due to the rapid subsequent
501 transformation via reaction with OH. Biogenically emitted compounds with high molar yields for the formation of
502 acetaldehyde are > C₂ alkenes (0.85) and ethanol (0.95). Additionally, isoprene and terpenes have a low molar yield
503 (0.019, 0.025) but exhibit the strongest emissions measured from the forest (Fischer et al., 2014). The reaction of other
504 aldehydes butanal, 2-pentanone, and 2-heptanone with OH and NO₃ also leads to the formation of acetaldehyde,
505 sometimes with high yields (Atkinson et al., 2000). In the data presented here, acetaldehyde at 80 m correlated best
506 with photolytically generated species like MVK, methacrolein, and C₅H₄O₃ (p = 0.96) and with benzaldehyde
507 (p = 0.93) in the dry season and correlated well with acetic acid (p > 0.92) in both seasons. In the transition season
508 correlations were weaker overall (Figs. 3–4), which could hint at different primary and secondary acetaldehyde
509 sources. Correlation coefficients of acetaldehyde and BC at 325 m were below 0.6 at daytime but at nighttime, in the
510 transition season, a rather high correlation with p = 0.82 was observed (Fig. S56).

511 From about 16:00 LT onwards until the next day the vertical gradient is reversed with the lowest concentrations at
512 80 m. This likely reflects the uptake to plant tissues regulated by compensation points since the NO₃ and O₃ reactivity
513 is rather low. Acetaldehyde exhibits the strongest observed loss rate at nighttime among all the carbonyl compounds
514 in the dry season and it had the highest Henry's law constant (Table 2).

515 4.2 Acetone

516 Acetone (propanone) is the simplest ketone and the most abundant and widespread OVOC in the atmosphere due to
517 its relatively long atmospheric lifetime of 15 days (Singh et al., 2004) (primarily driven by photolysis in the upper
518 troposphere, 119 days with respect to OH). The variation of acetone mixing ratios throughout the day above the
519 roughness sublayer at 150 and 325 m was small compared to the other carbonyls. However, mixing ratios at 80 m
520 increased substantially with light and temperature during the day. In the wet-to-dry transition season mixing ratios
521 reached 1.33, 1.12, 1.15 ppb on average, while in the dry season, 2.55, 1.66, 1.71 ppb (80, 150, 325 m) were measured.

522 The vertical distribution of acetone showed clearly enhanced mixing ratios at 80 m during daytime compared to well-
523 mixed conditions at the higher altitudes sampling points. The strong gradient in the first 150 m above the canopy is
524 strong despite the low reactivity of acetone, which raised the question of how acetone is distributed vertically in the
525 roughness sublayer. indicated a large positive flux above the canopy. Possible reasons for this strong gradient include
526 primary biogenic emission, biomass burning, production from leaf wax, or efficient secondary formation from very
527 short lived precursors that exceed deposition and stomatal uptake. Flux measurements in a tropical forest in Costa

528 Rica in the dry season have found a bidirectional but net-positive canopy flux of acetone (Karl et al., 2004).
529 Additionally in 2013, when several carbonyls were measured at ATTO below 80 m, the acetone mixing ratios inside
530 the canopy (influenced by surrounding trees) were lower than the values measured at 79 m in the dry season. Both
531 studies deployed PTR-quadrupole-MS operated with H₃O⁺ reagent ions with a nominal mass resolution. As for
532 acetaldehyde, these increasing vertical gradients suggested a dominance of photolytically secondary formation over
533 direct emission. In the wet season in 2013, however, mixing ratios measured in the canopy and at 79 m were of similar
534 magnitude and, compared to the dry season, much lower at both heights. In conclusion, no clear dominance of
535 secondary formation or direct emission was found in the wet season (Yáñez-Serrano et al., 2015). We also observed
536 seasonal differences at all three heights, with lower mixing ratios in the transition compared to the dry season. While
537 we cannot report acetone observations from the wet season, we did observe higher correlations of acetone with non-
538 primary emitted OVOC methacrolein, MVK, and C₃H₄O₃ in the transition season ($p > 0.82$) compared to the dry
539 season, suggesting that in 2019 secondary formation contributed more acetone to observed mixing ratios in the
540 transition season than in the dry season. In light of the widely differing atmospheric lifetimes of acetone and those
541 OVOC, the most likely explanations for the high transition season correlations is a dominating secondary acetone
542 source at a similar rate or similar surface uptake. Contributions from aged biomass burning plumes containing acetone
543 in the dry season, when enhanced BC concentrations were observed, could also be the reason for a weaker correlation
544 of C₃H₄O₃, methacrolein, and MVK with acetone in the dry season. Based on the information obtained in 2013 and
545 the data observations from this study, secondary production in the dry and transition season appears to peak between
546 the canopy and 150 m above ground above the canopy, adding up to varying contributions of direct emissions and
547 uptake from by vegetation. It is thus possible that strong secondary formation competes with uptake by vegetation to
548 generate a local maximum in the rough surface layer, which is observed in this study by the enhanced mixing ratios
549 observed at 80 m. Sweeps and ejections in and out of the canopy in the roughness sublayer could make the uptake of
550 acetone by different vegetation species and soils very efficient. The strong gradient between 80 and 150 m likely
551 reflects an acetone peak in the vertical. In conclusion, the most relevant precursors were very reactive biogenic
552 compounds. The best correlations were found with MEK ($p > 0.87$) in both seasons, which is another long-lived ketone
553 that is known to be directly emitted from the Amazon rainforest and produced in the atmosphere overhead (Yáñez-
554 Serrano et al., 2015, 2016).

555 Primary sources of acetone are direct emission from vegetation and, to a smaller extent, also from dead plant matter.
556 Acetone is released during cyanogenesis, which acts as a repellent that stops herbivores eating the plant's leaves.
557 During the production and release of volatile hydrogen cyanide, which deters the feeding herbivore, acetone is formed
558 as a byproduct. Cyanogenesis occurs in many plant species, though some employ different mechanisms to produce
559 hydrogen cyanide so that other carbonyl byproducts can be released (Fall, 2003). Another known biogenic pathway
560 for acetone formation is acetoacetate decarboxylation in soil bacteria and humans (Fall, 2003). Both light and
561 temperature have been suspected to drive acetone emissions, as shown for some pine and spruce trees (Seco et al.,
562 2007).

563 Secondary formation of acetone is known to occur from anthropogenically emitted C₃-C₅ isoalkanes (propane,
564 isobutane, isopentane) and biogenic emitted methyl butenol and certain terpenes (Fischer et al., 2014; Jacob et al.,
565 2002; Seco et al., 2007). We found mixing ratios of isopentane to be below the detection limit (13 ppt), and the vertical
566 distribution and correlations reported for acetone indicated a rapid formation in the first 150 m above ground rough
567 surface layer by hydrocarbons that are much more short-lived than alkanes. The ozonolysis of compounds in
568 epicuticular leaf waxes constitutes another source of acetone as mentioned in section 3.3.

569 At night, deposition could be observed on the basis of the rapidly decreasing mixing ratios at 80 m, compared to the
570 slowly occurring reactions with NO₃ and O₃. Similar effects have been reported in flux measurements performed by
571 Karl et al. (2004).

572 **4.3 Propanal**

573 Propanal is an isomer of acetone and is not distinguishable from acetone by classical PTR-MS type instruments using
574 H₃O⁺. In this study, the first high temporal resolution measurements of propanal in a tropical forest are presented, and
575 the vertical distribution above the canopy was found to differ markedly from acetone. In general, in the remote
576 atmosphere, we may expect the more reactive propanal to have lower mixing ratios than acetone, although this may

577 not be true close to sources. We measured average concentrations of 176, 150, and 119 ppt in the wet-to-dry transition
578 and 165, 115, and 85 ppt in the dry season (80, 150, 325 m). The ratio of propanal to acetone in the roughness sublayer
579 of the tropical forest and above yields 1:7.6, 1:9.6 (transition season) and 1:15.4, 1:20 (dry season) at 80 and 325 m.
580 Globally, the mixing ratio of propanal has been estimated to be about one-third of acetaldehyde (Singh et al., 2004),
581 while at ATTO a ratio of 1:4.2, 1:8.1 (transition season) and 1:7.2, 1:14 (dry season) was measured at 80 and 325 m,
582 respectively. However, it should be noted that, globally, a large propanal source is propane oxidation, which is
583 predominantly emitted from anthropogenic activities associated with oil and gas use. Acetaldehyde sources in the
584 rainforest thus far exceed propanal sources in the context of the global budget (Warneck, P.; Williams, J., 2012).

585 Propanal emission from vegetation has been reported for non-tropical forests (Guenther, 2000; Villanueva-Fierro et
586 al., 2004), although the metabolic pathway was not specified. Wang et al. (2019) described the biosynthesis of
587 acetaldehyde and propanal during fruit ripening. It was also noted that propanal emission occurs from ferns (Isidorov
588 et al., 1985), which is important since fern species are common in the understory of tropical forests.

589 Throughout the day, propanal exhibited a negative vertical gradient (i.e., decreasing mixing ratio with increasing
590 height). This occurs most likely due to dilution and photochemical loss of propanal generated in or emitted from the
591 canopy. A similar distribution was also observed for monoterpenes and isoprene, which are primary emitted VOC.
592 Accordingly, propanal observed at 80 m also correlates best with isoprene in both seasons ($0.89 > p > 0.98$) followed
593 by monoterpenes ($0.84 > p > 0.92$). The estimated atmospheric lifetime of propanal of about 1 day (Guimbaud et al.,
594 2007) (1.2 days for the oxidation by OH, table 2) is similar to that of acetaldehyde, but the vertical profiles revealed
595 different distributions in the first 325 m above ground (Figures 1 and 2). The weak gradient of acetaldehyde between
596 150 and 325 m at daytime in contrast to the steadily decreasing vertical profile of propanal can thus only be explained
597 by a higher yield of acetaldehyde from secondary production above 150 m. This is not surprising since acetaldehyde
598 is produced during oxidative degradation of many hydrocarbons. The secondary production of propanal is known to
599 occur via the photochemical oxidation of C₃ and larger hydrocarbons (Singh et al., 2004) and propane (Altshuller,
600 1991). Their lifetimes range from 5 days to a few hours (Altshuller, 1991). However, due to the high correlation of
601 propanal and isoprene, which is even higher than the correlation of isoprene and its oxidation products MVK and
602 methacrolein, a primary and mainly light-dependent source is surmised.

603 Nighttime mixing ratios of propanal were decreasing at 80 m (Table 2). Since the reaction rate of propanal with NO₃
604 is faster and the water solubility lower than that of the other carbonyl compounds, a higher fraction could potentially
605 react in the atmosphere. Stomatal uptake for the terpenes might be driven by the concentration gradient between leaf
606 and atmosphere, and the same might hold for propanal.

607 **4.4 Methyl Ethyl Ketone (MEK)**

608 Mixing ratios of MEK in the wet-to-dry transition were 177, 175, and 177 ppt on average, compared to 249, 188, and
609 185 ppb in the dry season (80, 150, 325 m). With a conventional PTR-MS, butanal and MEK are detected at the same
610 exact mass, whereas in this study using NO⁺ reagent ions solely MEK was measured. Butanal mixing ratios were
611 determined to be below the detection limit (20 ppt); thus, the contribution of butanal to MEK for PTR-MS can be
612 assumed to be very low. The mixing ratios obtained in this study agree well with previous studies conducted with a
613 PTR-quadrupole-MS at the ATTO site in 2013 and close to Manaus (Amazonia) in 2014, which would not completely
614 exclude possible interferences on the nominal mass of MEK (Yáñez-Serrano et al., 2015, 2016). The vertical
615 distribution of MEK throughout the day resembles that of acetone in both seasons. Mixing ratios above the roughness
616 layer (at 150 and 325 m) were almost uniform, while those at 80 m showed a more pronounced diurnal cycle with
617 strongly increasing values in the day and decreasing values at night. As well as being structurally similar to acetone,
618 MEK also has a long lifetime of 4.3 days (Fischer et al., 2014) (19.3 with respect to OH oxidation alone) relative to
619 mixing timescales. MEK is also known to have primary and secondary sources (Yáñez-Serrano et al., 2016) and to be
620 uptaken by vegetation (Edtbauer et al., 2021; Tani et al., 2013). Therefore, it is not surprising that MEK correlated
621 best with acetone at 80 m ($p = 0.87$ in the dry season), but in the transition season, it also correlated well with C₅H₄O₃,
622 methacrolein, and MVK. This suggests secondary sources from biogenically emitted precursors were more dominant
623 during the transition season than in the dry season, similar to acetone.

624 MEK emissions have been reported for rainforest canopies (Yáñez-Serrano et al., 2015) and fern (Isidorov et al.,
625 1985), decaying plant matter (Warneke et al., 1999), fungi, and bacteria (Yáñez-Serrano et al., 2016). The metabolic
626 pathways of production and the release mechanisms are poorly understood but have been suggested to involve plant
627 signaling, injured leaves, and root-aphid interactions (Yáñez-Serrano et al., 2016). Within-plant conversion of the
628 cytotoxic 1,2-ISOPOOH, which was deposited on poplar leaves, first to MVK and subsequently to MEK, has been
629 reported to represent a large biogenic source of MEK. The enzyme responsible for the conversion of MVK to MEK
630 is widespread among plants (Canaval et al., 2020).

631 The secondary formation of MEK occurs via the oxidation of n-butane with a yield of 80% (Singh et al., 2004) and
632 via oxidation of 2-butanol, 3-methyl pentane, and 2-methyl-1-butene (Yáñez-Serrano et al., 2016). Additionally, all
633 alkenes with a methyl/ethyl group on the same side of the olefin bond are possible precursors of MEK (Singh et al.,
634 2004). Butane was not expected to be abundant in the rainforest environment due to its anthropogenic sources, and
635 butane oxidation would also yield butanal, which was only detected below the LOD. As for acetone, the vertical
636 distribution and correlations discussed above suggest higher levels of short-lived precursors of MEK than of alkanes.

637 Rapidly decreasing concentrations at 80 m at night are in agreement with earlier studies, that reported deposition of
638 MEK in the canopy due to its high water solubility (Yáñez-Serrano et al., 2016) (Table 2).

639 **4.5 Methyl Vinyl Ketone and Methacrolein/2-Butenal**

640 The main source of both carbonyls MVK and methacrolein is the oxidation of isoprene by OH. Thus, they are
641 summarized in one section. It has been shown previously that methacrolein is detected together with 2-butenal (Koss
642 et al., 2016), which is also found in vegetation emission studies, albeit in small concentrations (Hellén et al., 2004;
643 Isidorov et al., 1985). (E)-2-butenal is a signaling compound within the plant that serves to trigger responses to abiotic
644 stress (Yamauchi et al., 2015). Its atmospheric lifetime is around 20 hours, slightly longer than the lifetimes of
645 methacrolein and MVK which are 10 and 14 hours, respectively (Hellén et al., 2004; Liu et al., 2016). It is also known
646 that MVK and methacrolein cannot be detected separately from isoprene hydroxyhydroperoxides (ISOPOOH) without
647 using a scrubber, since the hydroperoxides decompose onto the same m/z. With NO⁺ CIMS the fragment of 1,2-
648 ISOPOOH and methacrolein share one m/z-ratio, while 4,3-ISOPOOH is detected together with MVK (Rivera-Rios
649 et al., 2014). Wall exchange effects in the inlet line might have led to the removal of ISOPOOH from the sampled air
650 due to their reduced volatility, but a contribution to the MVK and methacrolein signal remains possible. ISOPOOH
651 also originate from the oxidation of isoprene and are very reactive, reflected by lifetimes of 3 and 2 hours. After the
652 initial reaction of OH and isoprene, the subsequently formed peroxy radical (RO₂) can react with NO to form MVK
653 and methacrolein, but it can also react with HO₂ to form ISOPOOH (Liu et al., 2016). At close to pristine conditions
654 at ATTO, NO mixing ratios are low, and the yield distribution between ISOPOOH, MVK, and methacrolein was
655 estimated to be 50, 25, and 25%, respectively (Ringsdorf et al., 2023; Rivera-Rios et al., 2014). It has been shown that
656 the oxidation of isoprene can proceed already within plant tissues by reaction with accumulated reactive oxygen
657 species. The accumulation of reactive oxygen species, including OH, is a reaction to biotic and abiotic stresses and
658 can exceed the antioxidant defense capacities in the tissue. The oxidation of isoprene within the tissue reduces the
659 amount of reactive oxidized species and leads to the direct emission of isoprene's products MVK and methacrolein,
660 especially under stress (Jardine et al., 2012b, 2013).

661 Oxidation of the monoterpene ocimene has been identified as another secondary source for MVK (Calogirou et al.,
662 1999). To our knowledge, there are no other significant direct or secondary sources of MVK, methacrolein, and
663 ISOPOOH other than the oxidation of isoprene. This explains the observed diurnal cycle with an afternoon maximum
664 due to the light-dependent emission of isoprene and the photochemical production of OH. Since isoprene is present at
665 relatively high mixing ratios at all tree sampling heights (3.69, 3.33, 3.0 ppb at 80, 150, and 325 m in the dry season),
666 the oxidative formation of MVK, methacrolein, and ISOPOOH takes place throughout the mixed layer. The observed
667 slightly increasing mixing ratios of MVK with height are consistent with rapid isoprene oxidation above the canopy,
668 slower removal of MVK itself, and turbulent in-mixing of cleaner air from above. Isoprene has an estimated
669 atmospheric lifetime of about 3 hours, and it was previously reported that only circa 10% of emitted isoprene was
670 oxidized within the canopy (Karl et al., 2004). Unlike MVK, methacrolein and 2-butenal show a slightly decreasing
671 vertical gradient. Sources and sinks of MVK and methacrolein are very closely related, so the presence of significant
672 quantities of 2-butenal is the most likely explanation for that difference.

673 Dry deposition to leaf surfaces has been observed in a previous study for the sum of MVK and methacrolein and
674 individually for these compounds during daytime (Nguyen et al., 2015; Tani et al., 2010). Uptake by leaves represents
675 a significant sink that exceeds loss via OH oxidation near leaves (Tani et al., 2010). In this study, the rapid decrease
676 of nocturnal concentrations at 80 m indicated that deposition at night was also taking place.

677 MVK and methacrolein + 2-butenal showed similar mixing ratios in the dry season of 607, 599, 659 ppt MVK and
678 679, 644, 644 ppt methacrolein + 2-butenal. It has to be considered that the uncertainty of MVK mixing ratios is higher
679 than the uncertainty of methacrolein mixing ratios due to their k-rate-based calculation rather than calibration to a gas
680 standard. In the transition season, methacrolein + 2-butenal (415, 425, 439 ppt) exceeded the mixing ratios of MVK
681 (184, 229, 265 ppt). Whether that resulted from the high seasonal variability of 2-butenal or from the contribution of
682 ISOPOOH, unfortunately, remains unclear. Lower levels of all isoprene oxidation products were expected as a result
683 of lower isoprene mixing ratios and photo-oxidation rates in the transition season.

684 **4.6 Sum of C₅-ketones**

685 The mixing ratios obtained for the sum of C₅-ketones were 11, 9, and 9 ppt in the transition season, while slightly
686 higher levels of 14, 8, and 7 ppt (80, 150, 325 m) were obtained in the dry season. A diurnal cycle was observed at
687 80 m only, whereas levels at 150 and 325 m were similar and showed no trend throughout the day and night. C₅-
688 ketones were 2- and 3- pentanone as well as 3-methyl-2-butanone. The atmospheric lifetime of 2-pentanone is in the
689 range of 5 days. All three ketones have been included in emission inventories from plants (Isidorov et al., 1985;
690 Kesselmeier and Staudt, 1999; König et al., 1995), but there is little information on metabolic pathways or
691 mechanisms. 2-pentanone has been identified as a marker for fungal activity in indoor environments (Kalalian et al.,
692 2020), since it is produced in the hyphae of *Aspergillus niger* (Lewis, 1970), a fungus that was also found to degrade
693 biomass in the Amazon. 3-pentanone is one of the C₅ green leaf volatiles (GLV) emitted at lower rates than C₆ GLV,
694 which are described in the next section (Jardine et al., 2012a). An increase of 3-pentanone coincident with high
695 temperatures after noon was observed at another measurement station in the Amazon rainforest, with a simultaneous
696 decrease of terpenoid emissions (Jardine et al., 2015). Consistent with this observation, in this study, the correlation
697 of C₅ ketones with isoprene or monoterpenes was low in the transition and dry season during the daytime ($p < 0.39$).
698 The best correlations for C₅-ketones of $0.53 < p < 0.6$ were obtained with acetone and MEK. This was most likely a
699 consequence of common sources, including primary emission and formation from rather short-lived hydrocarbons and
700 of the long atmospheric lifetimes relative to mixing timescales, which the observed ketones have in common. Above
701 150 m, no diurnal variability was observed, which is also in agreement with the other ketones, suggesting they were
702 well-mixed above the Amazonian roughness sublayer. As suspected for acetone, the vertical distribution of C₅-ketones
703 might have been peaking around 80 m as a result of the bidirectional exchange in the canopy and secondary formation.

704 Fumigation experiments with different VOC have shown a loss of all three C₅-ketones on leaf surfaces (Tani and
705 Hewitt, 2009). A decrease of the mixing ratios at 80 m could be observed at nighttime, and a high water solubility of
706 the ketones indicated a high loss rate. However, the signal was too noisy to determine loss rates from the data.

707 C₅-aldehydes, which were usually detected together with the C₅-ketones, exhibited lower mixing ratios, especially in
708 the dry season. Overall, the mixing ratios were below their LOD and thus not investigated in detail. However, a diurnal
709 and vertical pattern of C₅-aldehydes with vertical and diurnal variabilities different to those of the C₅-ketones was still
710 apparent.

711

712 **4.7 n-Hexanal/Hexenols and Hexenals**

713 C₆-aldehydes, namely n-hexanal, Z-2-hexenal, Z-3-hexenal, E-2-hexenal, and E-3-hexenal, together with C₆-alcohols
714 and esters form a group that is often termed green leaf volatiles (GLV). Although different temporal variabilities were
715 observed for n-hexanal/hexenols and hexenals, we here discuss them together in one section due to their common
716 sources.

717 In the chloroplasts of almost all green plants, GLV are synthesized from fatty acids as part of the oxylipin pathway.
718 Their emission results from wounding or mechanical damage, from abiotic factors (such as wind), herbivores, and

719 pathogen attack (Scala et al., 2013). The amount of GLV emitted from corn plants has been shown to depend on soil
720 water content, temperature, light, and fertilization, with a stronger emission response at higher temperatures
721 (Gouinguéné and Turlings, 2002). Furthermore, emission has been reported as a response to abiotic stress from light–
722 dark transitions (Jardine et al., 2012a). Their production and release can be very fast; in the case of Z-3-hexenal,
723 emission begins only 1 or 2 seconds after damage (Fall et al., 1999). On one hand, GLV have antibiotic properties and
724 protect the wounded tissue from invading bacteria or other microorganisms. On the other hand, their rapid production
725 and release make them useful for intra and inter-chemical communication in plants, for example for priming defense
726 mechanisms. It has been found that a herbivore-infested plant releases signaling compounds, like GLV to attract the
727 predator (insects, beetles, birds, etc.) of the herbivore (Mumm and Dicke, 2010; Scala et al., 2013; Zannoni et al.,
728 2020a). The release of GLV can happen on short timescales of minutes to hours but in cases of repetitive wounding
729 or drying of leaves, the emission can be continuous over days (Fall et al., 1999; Scala et al., 2013). Release of GLV is
730 also caused by drought stress, and GLV levels have been observed to increase at noon as a result of high temperatures
731 in the Amazon forest (Jardine et al., 2015; Kesselmeier and Staudt, 1999).

732 It remains unclear if the leaf alcohol Z-3-hexanol contributed to the hexenal signal. Z-3-hexanol is also a GLV and
733 has been reported to represent a major part of the emission of many studied plants (Kesselmeier and Staudt, 1999). Its
734 atmospheric lifetime was calculated to be 5 hours with respect to OH. Further, the less abundant isomers, such as Z-
735 4-hexenol or E-2-hexenol, are also likely to contribute to the hexenal signal. Due to photolysis and reaction with OH,
736 the lifetime of n-hexenal is about 4 hours (12 hours for oxidation by OH only), which is also true for E-2-hexenal
737 (Jiménez et al., 2007). Z-3-hexenal has a shorter atmospheric lifetime of 3 hours (Xing et al., 2012).

738 At ATTO, the integrated emissions from a large uniform area were measured, which made it impossible to detect
739 single wounding events, except for large-scale storm damage or human activities such as forest clearing. Measured
740 mixing ratios were 15, 11, and 9 ppt for n-hexenal in the transition season and 26, 19, and 16 ppt in the dry season.
741 Hexenals were detected at mixing ratios below LOD (6 ppt) for most parts of the day in the transition season, and 8
742 ppt were measured at 80 m in the dry season. Nighttime mixing ratios of hexenals at 150 and 325 m were, however,
743 also below the LOD (6 ppt). During both measurement phases, n-hexenal was continuously present, exhibiting a
744 distinct diurnal cycle with maximum mixing ratios in the afternoon and higher values in the dry season. Since the
745 emission rate of damaged leaves of hexenals was found to be higher compared to n-hexenal (Fall et al., 1999), the
746 contribution of hexanols to the signal of n-hexenal was very likely. Average daytime mixing ratios between 40 and
747 70 ppt have also been observed for hexenal and/or hexenols in an elevated position above the rainforest of Malaysia
748 (Langford et al., 2010). To investigate whether the diurnal cycle results from temperature-dependent emission of GLV
749 or additional secondary formation, measurements inside the canopy are required.

750 It was not surprising that a continuous decrease in both n-hexenal and hexenols with height was observed throughout
751 the day, similar to propanal and other reactive primary emissions like isoprene and monoterpenes. Correlations at
752 80 m with isoprene ($0.78 < p < 0.86$), monoterpenes ($0.74 < p < 0.91$), and propanal ($p = 0.88$, dry season) indicated
753 light- or temperature-driven emission or rapid secondary formation close to the canopy. This correlation is interesting
754 since GLV emissions upon biotic-induced stresses such as herbivory do not necessarily follow a diel cycle. However,
755 boundary layer dynamics might have modulated the diel cycle since mixing between the canopy and atmosphere is
756 most efficient during daytime convective conditions. Additionally, temperature-related drying of leaves could have
757 led to the observed diel variability.

758 In contrast to n-hexenal/hexenols, hexenals exhibit a more pronounced seasonal variability, with very low mixing
759 ratios, mostly below the LOD, in the transition season. The correlation with isoprene and monoterpenes during the
760 daytime in the dry season was rather low ($p = 0.71$), with the highest correlations for acetone, MEK, benzaldehyde,
761 and ethanol ($p > 0.8$), suggesting primary and secondary sources of hexenals.

762 For all C₆-aldehydes investigated in this section, decreasing concentrations during nighttime at all three heights were
763 observed in the dry season, when C₆-aldehydes mixing ratios were generally higher than in the transition season. A
764 slightly slower decrease of 80-m mixing ratios compared to the higher levels in the dry season may indicate a continued
765 nocturnal emission of GLV, which is plausible since production and release from mechanical wounding, stress, or
766 herbivory is possible without light (He et al., 2021).

767 4.8 Benzaldehyde

768 The average mixing ratios of benzaldehyde measured in this study are 12, 12, 12 ppt in the transition season and 11,
769 10, 11 ppt (80, 150, 325 m) in the dry season. No seasonal variability or vertical gradient was observed between the
770 measurement periods.

771 Benzaldehyde is the lightest monoaromatic aldehyde and is formed via the oxidation of other aromatic compounds. It
772 is a major intermediate product of the oxidation of benzyl radicals via OH and, thereby, of all alkyl-substituted
773 aromatic hydrocarbons (Sebban et al., 2011). Biogenic aromatics, such as volatile benzenoids or larger molecules like
774 lignols, are produced via the shikimate pathway by plants, which is an important metabolic process, but benzaldehyde
775 can also be emitted by microorganisms (Ladino-Orjuela et al., 2016; Laothawornkitkul et al., 2009). The oxidation of
776 toluene, which has previously been observed to be emitted from forested environments and farm crops (Heiden et al.,
777 1999), yields benzaldehyde as a product (6-%) (Atkinson and Arey, 2003). Benzaldehyde is also a benzyl alcohol
778 oxidation product, which has been reported previously to be emitted from biogenic sources (Bernard et al., 2013).
779 Benzaldehyde is very reactive, with a calculated atmospheric lifetime primarily determined by its photolysis rate of
780 2.4 hours (Cabrera-Perez et al., 2016) (1.7 days with respect to OH).

781 Primary emission of benzaldehyde from vegetation has been reported for grass (Kirstine et al., 1998) and elevated
782 concentrations under and within the canopy of the Amazon rainforest were measured (Kesselmeier et al., 2000). The
783 high mixing ratios (about 300 ppt) found at the ground were suspected to result from the decomposition of biomass,
784 specifically the decomposition of lignols within the litter. In that study, the mixing ratios above the canopy were much
785 lower than those measured at ground level.

786 The apparent light or temperature-driven diurnal cycle of benzaldehyde suggests secondary photochemical production
787 from aromatic hydrocarbons, as the shikimate pathway is independent of light (Jan et al., 2021). The atmospheric
788 lifetime of precursor aromatics ranges from days to weeks (Altshuler, 1991). Secondary production from long-lived
789 precursors is a feasible explanation for the missing vertical variability of the very reactive benzaldehyde in the first
790 325 m of the mixed layer. The rather slow secondary production throughout the mixed layer possibly compensated
791 for the expected loss through oxidation and dilutive mixing. Mixing ratios observed at 80 m were only slightly more
792 abundant in the dry season compared to higher altitudes, which could mean a stronger contribution of benzaldehyde
793 emissions. However, the narrow vertical benzaldehyde distribution points towards well-mixed aromatic precursor
794 hydrocarbons. Daytime mixing ratios of carbonyls that are suspected to be formed predominantly due to
795 photochemical formation, namely, acetic acid, $C_3H_4O_3$, methacrolein, MVK, but also acetaldehyde and acetone,
796 correlate very well with benzaldehyde in the dry season ($0.85 > p > 0.95$). In the transition season, the correlation with
797 the same compounds is smaller ($0.75 > p > 0.86$). Possible explanations for this difference most likely lie in altered
798 sources of precursors or benzaldehyde itself due to differences in, e.g., litter decomposing activities. It is important to
799 note that the missing vertical variability could also be a sign of contamination from the measurement tower itself, e.g.,
800 through temperature-dependent outgassing of its coating. However, the measurement of the fresh paint did not show
801 elevated benzaldehyde, while the fresh anticorrosion agent emits some benzaldehyde, but at much lower rates than
802 other VOC, e.g., toluene or xylene.

803 Globally, dry deposition constitutes a small sink of benzaldehyde in the same range as oxidation by NO_3 (Cabrera-
804 Perez et al., 2016). We observed decreasing mixing ratios at all three heights throughout the night (Table 2). Wet
805 deposition and uptake to leaves and soil might have been the dominant sink.

806 There is evidence that benzaldehyde PAN can emerge when transported to high NO_x regions (Caralp et al., 1999).
807 Mixing ratios of PAN are quite high so this must be considered, but photochemical PAN creation potential is the
808 lowest of the whole group of organic compounds (Derwent et al., 1998).

809

810 5 Conclusion

811 In this study, a PTR-ToF-MS was operated using NO^+ as the reagent ion for measuring specific carbonyl compounds
812 at three heights (80, 150, 325 m), in two seasons, and over 24-hour cycles, on the ATTO tower located in the Brazilian
813 Amazon rainforest. With the more commonly used ionization method for PTR-MS involving H_3O^+ ions, aldehyde and
814 ketone isomers were detected together at the same exact mass. This precludes the investigation of the individual
815 species. For the first time, mixing ratios of biogenic aldehydes and ketones measured at high frequency are reported
816 for a rainforest ecosystem. Generally, higher mixing ratios were found in the dry season. To some extent, this can be
817 attributed to higher temperatures and enhanced light conditions, which drive emissions and photochemical activity.
818 However, since temperature and PAR were only slightly enhanced in the dry season compared to the wet-to-dry
819 transition, other aspects such as phenology (gross ecosystem productivity peaking in the dry season) and contribution
820 of long-lived species from aged biomass burning plumes are of importance. Ketones have atmospheric lifetimes (days
821 to weeks) that are much longer than the vertical mixing times (15–60 min) (Ringsdorf et al., 2023). Such compounds
822 can, therefore, be expected to be also present above the lowermost mixing layer (ABL) in the residual layer and free
823 troposphere. Interestingly, elevated ketone mixing ratios in the roughness sublayer observed at 80 m by day suggest a
824 large source ~~above or at~~ canopy level, balanced with a surface uptake process. To examine these strong vertical
825 gradients observed for some ketones, continuous measurements with altitude are planned using a PTR-ToF-MS
826 installed on an elevator attached to the tower. -This system will allow investigation of the exchange of VOC between
827 canopy and atmosphere and reveal whether mixing ratios of acetone, MEK and C₅-ketones are peaking around 80 m
828 as suggested by the observed elevated mixing ratios at 80 m or just above. At night, the loss of these species indicates
829 a rapid deposition to the canopy or the underlying forest floor. The correlations shown in Figures 3–4 reveal seasonal
830 differences in the partitioning of primary emission from the canopy and the rate of rapid secondary production above
831 the canopy. The most abundant individually measured carbonyls in this study were acetaldehyde and acetone, both
832 effective PAN precursors, followed by isoprene oxidation products and propanal. Note that formaldehyde was not
833 detected by the applied method. The shorter-lived, longer-chain aldehydes observed in this study showed great
834 variation, exhibiting both increasing and decreasing vertical gradients that vary considerably in strength. All carbonyl
835 compounds showed a distinct diurnal cycle which followed the evolution of light and temperature during the day and,
836 for most compounds, a decrease during the night driven in part by reaction with NO_3 but more importantly by
837 deposition to plant tissues, as has been shown by flux measurements for a few oxygenated species before (Karl et al.,
838 2004). The nocturnal uptake of these carbonyl compounds is an important aspect of their local-to-regional-scale
839 budget. Based on this data, we hypothesize that the ecosystem can more efficiently produce reduced species such as
840 isoprene and monoterpenes but more efficiently utilize the oxygenated products of these precursors. The importance
841 of uptake followed by metabolization or storage, especially for oxygenated BVOC has been stressed already in the
842 context of bidirectional exchange of BVOC by Niinemets et al. (2014). This would imply that the rainforest exploits
843 atmospheric oxidation to convert products into more useful, metabolizable forms. Similar preferences for the uptake
844 of oxygenated species over terpenes have been reported for epiphytes such as lichen and moss (Edtbauer et al., 2021).
845 This idea can serve as the basic hypothesis for future plant experiments and the observed loss rates of carbonyl species
846 can help to constrain turbulence resolving canopy exchange models. Overall, we need to improve our understanding
847 of the complexity of biological production and consumption and invest into investigations of primary emissions on a
848 leaf or branch level.

849 Butanal, and carbonyls higher than C_7 were found to be minor components of the rainforest atmosphere, as were the
850 alkanes isopentane, methylcyclopentane, sum of 2- and 3-methylpentane and C_7 cyclic alkanes. The ratio of the
851 aldehydes propanal and acetaldehyde, which have comparable atmospheric lifetimes and which were shown to
852 correlate very well in previous studies, was found to be much higher with 1:4.2 and 1:7.2 in the transition and dry
853 season at 80 m compared to the global average ratio of 1:3 (Singh et al., 2004), due to the overwhelming predominance
854 of biogenic sources and precursors in the rainforest.

855 This application of the NO^+ CIMS method has enabled the study of the individual carbonyls not accessible using the
856 H_3O^+ -based method. We, therefore, recommend periodic switching of the reagents to allow for more specific detection
857 of biogenic emissions. This would complement long-term measurements conducted using the H_3O^+ ionization method.

858

859 **Code availability.** The python code can be provided upon request.

860 **Data availability.** BVOC datasets are available on the ATTO data portal (<https://www.attodata.org/>), a DOI is
861 ~~requested and will follow soon~~ <https://doi.org/10.17871/atto.355.4.1493>, <https://doi.org/10.17871/atto.354.3.1494>,
862 <https://doi.org/10.17871/atto.353.7.1495> and <https://doi.org/10.17871/atto.352.7.1496>. -Meteorological data
863 conducted at the ATTO tower (320 m) in 2019 are available via <https://doi.org/10.17871/atto.95.12.742>.

864 **Supplement link:** A link to the supplement will be included by Copernicus, if applicable.

865 **Author contributions:** AR and AE conducted the BVOC measurements and AR analyzed this data and drafted the
866 manuscript. BH and CP provided the black carbon observations and meteorological parameters conducted at the
867 325-m-tall tower. MOS and AA conducted the measurements of the meteorological parameters at the 80 m tower.
868 J.W. supervised this study. J.L. supervised the research that led to this study.

869 **Competing interests:** The authors declare that they have no conflict of interest.

870 **Acknowledgements:** We acknowledge the support by the German Federal Ministry of Education and Research
871 (BMBF contract 01LB1001A and 01LK1602B) and the Brazilian Ministério da Ciência, Tecnologia e Inovação
872 (MCTI/FINEP contract 01.11.01248.00) as well as the Amazon State University (UEA), FAPESP, CNPq, FAPEAM,
873 LBA/INPA, and SDS/CEUC/RDS-Uatumã. We thank Thomas Klüpfel for his help with VOC measurements. We
874 especially acknowledge the technical and logistical support of the ATTO team (in particular Reiner Ditz and Hermes
875 Braga Xavier). We also thank Andrew Crozier for creating and providing a detailed map of the ATTO site.

876 **6 References**

877 Altshuler, A. P.: Chemical reactions and transport of alkanes and their products in the troposphere, *J. Atmospheric*
878 *Chem.*, 12, 19–61, <https://doi.org/10.1007/BF00053933>, 1991.

879 Andreae, M. O.: Emission of trace gases and aerosols from biomass burning – an updated assessment, *Atmospheric*
880 *Chem. Phys.*, 19, 8523–8546, <https://doi.org/10.5194/acp-19-8523-2019>, 2019.

881 Andreae, M. O. and Merlet, P.: Emission of trace gases and aerosols from biomass burning, *Glob. Biogeochem.*
882 *Cycles*, 15, 955–966, <https://doi.org/10.1029/2000GB001382>, 2001.

883 Andreae, M. O., Artaxo, P., Brandão, C., Carswell, F. E., Ciccioli, P., da Costa, A. L., Culf, A. D., Esteves, J. L.,
884 Gash, J. H. C., Grace, J., Kabat, P., Lelieveld, J., Malhi, Y., Manzi, A. O., Meixner, F. X., Nobre, A. D., Nobre, C.,
885 Ruivo, M. d. L. P., Silva-Dias, M. A., Stefani, P., Valentini, R., von Jouanne, J., and Waterloo, M. J.: Biogeochemical
886 cycling of carbon, water, energy, trace gases, and aerosols in Amazonia: The LBA-EUSTACH experiments, *J.*
887 *Geophys. Res. Atmospheres*, 107, LBA 33-1-LBA 33-25, <https://doi.org/10.1029/2001JD000524>, 2002.

888 Andreae, M. O., Acevedo, O. C., Araújo, A., Artaxo, P., Barbosa, C. G. G., Barbosa, H. M. J., Brito, J., Carbone, S.,
889 Chi, X., Cintra, B. B. L., da Silva, N. F., Dias, N. L., Dias-Júnior, C. Q., Ditas, F., Ditz, R., Godoi, A. F. L., Godoi,
890 R. H. M., Heimann, M., Hoffmann, T., Kesselmeier, J., Könemann, T., Krüger, M. L., Lavric, J. V., Manzi, A. O.,
891 Lopes, A. P., Martins, D. L., Mikhailov, E. F., Moran-Zuloaga, D., Nelson, B. W., Nölscher, A. C., Santos Nogueira,
892 D., Piedade, M. T. F., Pöhlker, C., Pöschl, U., Quesada, C. A., Rizzo, L. V., Ro, C.-U., Ruckteschler, N., Sá, L. D. A.,
893 de Oliveira Sá, M., Sales, C. B., dos Santos, R. M. N., Saturno, J., Schöngart, J., Sörgel, M., de Souza, C. M., de
894 Souza, R. A. F., Su, H., Targhetta, N., Tóta, J., Trebs, I., Trumbore, S., van Eijck, A., Walter, D., Wang, Z., Weber,
895 B., Williams, J., Winderlich, J., Wittmann, F., Wolff, S., and Yáñez-Serrano, A. M.: The Amazon Tall Tower
896 Observatory (ATTO): overview of pilot measurements on ecosystem ecology, meteorology, trace gases, and aerosols,
897 *Atmospheric Chem. Phys.*, 15, 10723–10776, <https://doi.org/10.5194/acp-15-10723-2015>, 2015.

898 Atkinson, R. and Arey, J.: Atmospheric Degradation of Volatile Organic Compounds, *Chem. Rev.*, 103, 4605–4638,
899 <https://doi.org/10.1021/cr0206420>, 2003.

900 Atkinson, R., Tuazon, E. C., and Aschmann, S. M.: Atmospheric Chemistry of 2-Pentanone and 2-Heptanone,
901 *Environ. Sci. Technol.*, 34, 623–631, <https://doi.org/10.1021/es9909374>, 2000.

902 Bernard, F., Magneron, I., Eyglunent, G., Daële, V., Wallington, T. J., Hurley, M. D., and Mellouki, A.: Atmospheric
903 Chemistry of Benzyl Alcohol: Kinetics and Mechanism of Reaction with OH Radicals, *Environ. Sci. Technol.*, 47,
904 3182–3189, <https://doi.org/10.1021/es304600z>, 2013.

905 Bond, D. W., Steiger, S., Zhang, R., Tie, X., and Orville, R. E.: The importance of NO_x production by lightning in
906 the tropics, *Atmos. Environ.*, 36, 1509–1519, [https://doi.org/10.1016/S1352-2310\(01\)00553-2](https://doi.org/10.1016/S1352-2310(01)00553-2), 2002.

907 Bourtsoukidis, E., Behrendt, T., Yañez-Serrano, A. M., Hellén, H., Diamantopoulos, E., Catão, E., Ashworth, K.,
908 Pozzer, A., Quesada, C. A., Martins, D. L., Sá, M., Araujo, A., Brito, J., Artaxo, P., Kesselmeier, J., Lelieveld, J., and
909 Williams, J.: Strong sesquiterpene emissions from Amazonian soils, *Nat. Commun.*, 9, 2226,
910 <https://doi.org/10.1038/s41467-018-04658-y>, 2018.

911 Bracho-Nunez, A., Knothe, N. M., Costa, W. R., Maria Astrid, L. R., Kleiss, B., Rottenberger, S., Piedade, M. T. F.,
912 and Kesselmeier, J.: Root anoxia effects on physiology and emissions of volatile organic compounds (VOC) under
913 short-and long-term inundation of trees from Amazonian floodplains, *SpringerPlus*, 1, 9, <https://doi.org/10.1186/2193-1801-1-9>, 2012.

915 Breuninger, C., Meixner, F. X., and Kesselmeier, J.: Field investigations of nitrogen dioxide (NO₂) exchange between
916 plants and the atmosphere, *Atmospheric Chem. Phys.*, 13, 773–790, <https://doi.org/10.5194/acp-13-773-2013>, 2013.

917 Brown, S. S. and Stutz, J.: Nighttime radical observations and chemistry, *Chem. Soc. Rev.*, 41, 6405,
918 <https://doi.org/10.1039/c2cs35181a>, 2012.

919 Cabrera-Perez, D., Taraborrelli, D., Sander, R., and Pozzer, A.: Global atmospheric budget of simple monocyclic
920 aromatic compounds, *Atmospheric Chem. Phys.*, 16, 6931–6947, <https://doi.org/10.5194/acp-16-6931-2016>, 2016.

921 Calogirou, A., Larsen, B. R., and Kotzias, D.: Gas-phase terpene oxidation products: a review, *Atmos. Environ.*, 33,
922 1423–1439, [https://doi.org/10.1016/S1352-2310\(98\)00277-5](https://doi.org/10.1016/S1352-2310(98)00277-5), 1999.

923 Canaval, E., Millet, D. B., Zimmer, I., Nosenko, T., Georgii, E., Partoll, E. M., Fischer, L., Alwe, H. D., Kulmala, M.,
924 Karl, T., Schnitzler, J.-P., and Hansel, A.: Rapid conversion of isoprene photooxidation products in terrestrial plants,
925 *Commun. Earth Environ.*, 1, 1–9, <https://doi.org/10.1038/s43247-020-00041-2>, 2020.

926 Cappellin, L., Karl, T., Probst, M., Ismailova, O., Winkler, P. M., Soukoulis, C., Aprea, E., Märk, T. D., Gasperi, F.,
927 and Biasioli, F.: On Quantitative Determination of Volatile Organic Compound Concentrations Using Proton Transfer
928 Reaction Time-of-Flight Mass Spectrometry, *Environ. Sci. Technol.*, 46, 2283–2290,
929 <https://doi.org/10.1021/es203985t>, 2012.

930 Caralp, F., Foucher, V., Lesclaux, R., Wallington, T. J., and Hurley, M. D.: Atmospheric chemistry of benzaldehyde:
931 UV absorption spectrum and reaction kinetics and mechanisms of the C₆H₅C(O)O₂ radical, *Phys. Chem. Chem.*
932 *Phys.*, 1, 3509–3517, <https://doi.org/10.1039/a903088c>, 1999.

933 Chamecki, M., Freire, L. S., Dias, N. L., Chen, B., Dias-Junior, C. Q., Machado, L. A. T., Sörgel, M., Tsokankunku,
934 A., and Araújo, A. C. de: Effects of Vegetation and Topography on the Boundary Layer Structure above the Amazon
935 Forest, *J. Atmospheric Sci.*, 77, 2941–2957, <https://doi.org/10.1175/JAS-D-20-0063.1>, 2020.

936 Chaparro-Suarez, I. G., Meixner, F. X., and Kesselmeier, J.: Nitrogen dioxide (NO₂) uptake by vegetation controlled
937 by atmospheric concentrations and plant stomatal aperture, *Atmos. Environ.*, 45, 5742–5750,
938 <https://doi.org/10.1016/j.atmosenv.2011.07.021>, 2011.

939 Chen, Y., Yuan, B., Wang, C., Wang, S., He, X., Wu, C., Song, X., Huangfu, Y., Li, X.-B., Liao, Y., and Shao, M.:
940 Online measurements of cycloalkanes based on NO⁺ chemical ionization in proton transfer reaction time-of-flight

- 941 mass spectrometry (PTR-ToF-MS), *Atmospheric Meas. Tech.*, 15, 6935–6947, [https://doi.org/10.5194/amt-15-6935-](https://doi.org/10.5194/amt-15-6935-2022)
942 2022, 2022.
- 943 Chevuturi, A., Klingaman, N. P., Rudorff, C. M., Coelho, C. A. S., and Schöngart, J.: Forecasting annual maximum
944 water level for the Negro River at Manaus, *Clim. Resil. Sustain.*, 1, e18, <https://doi.org/10.1002/cli2.18>, 2022.
- 945 Ciccioi, P., Silibello, C., Finardi, S., Pepe, N., Ciccioi, P., Rapparini, F., Neri, L., Fares, S., Brilli, F., Mircea, M.,
946 Magliulo, E., and Baraldi, R.: The potential impact of biogenic volatile organic compounds (BVOCs) from terrestrial
947 vegetation on a Mediterranean area using two different emission models, *Agric. For. Meteorol.*, 328, 109255,
948 <https://doi.org/10.1016/j.agrformet.2022.109255>, 2023.
- 949 Colomb, A., Williams, J., Crowley, J., Gros, V., Hofmann, R., Salisbury, G., Klüpfel, T., Kormann, R., Stickler, A.,
950 Forster, C., and Lelieveld, J.: Airborne Measurements of Trace Organic Species in the Upper Troposphere Over
951 Europe: the Impact of Deep Convection, *Environ. Chem.*, 3, 244–259, <https://doi.org/10.1071/EN06020>, 2006.
- 952 Deming, B. L., Pagonis, D., Liu, X., Day, D. A., Talukdar, R., Krechmer, J. E., de Gouw, J. A., Jimenez, J. L., and
953 Ziemann, P. J.: Measurements of delays of gas-phase compounds in a wide variety of tubing materials due to gas–
954 wall interactions, *Atmospheric Meas. Tech.*, 12, 3453–3461, <https://doi.org/10.5194/amt-12-3453-2019>, 2019.
- 955 Derwent, R. G., Jenkin, M. E., Saunders, S. M., and Pilling, M. J.: Photochemical ozone creation potentials for organic
956 compounds in northwest Europe calculated with a master chemical mechanism, *Atmos. Environ.*, 32, 2429–2441,
957 [https://doi.org/10.1016/S1352-2310\(98\)00053-3](https://doi.org/10.1016/S1352-2310(98)00053-3), 1998.
- 958 Edtbauer, A., Pfannerstill, E. Y., Pires Florentino, A. P., Barbosa, C. G. G., Rodriguez-Caballero, E., Zannoni, N.,
959 Alves, R. P., Wolff, S., Tsokankunku, A., Aptroot, A., de Oliveira Sá, M., de Araújo, A. C., Sörgel, M., de Oliveira,
960 S. M., Weber, B., and Williams, J.: Cryptogamic organisms are a substantial source and sink for volatile organic
961 compounds in the Amazon region, *Commun. Earth Environ.*, 2, 1–14, <https://doi.org/10.1038/s43247-021-00328-y>,
962 2021.
- 963 Ernle, L., Wang, N., Bekö, G., Morrison, G., Wargocki, P., J. Weschler, C., and Williams, J.: Assessment of aldehyde
964 contributions to PTR-MS m/z 69.07 in indoor air measurements, *Environ. Sci. Atmospheres*, 3, 1286–1295,
965 <https://doi.org/10.1039/D3EA00055A>, 2023.
- 966 Fall, R.: Abundant Oxygenates in the Atmosphere: A Biochemical Perspective, *Chem. Rev.*, 103, 4941–4952,
967 <https://doi.org/10.1021/cr0206521>, 2003.
- 968 Fall, R., Karl, T., Hansel, A., Jordan, A., and Lindinger, W.: Volatile organic compounds emitted after leaf wounding:
969 On-line analysis by proton-transfer-reaction mass spectrometry, *J. Geophys. Res. Atmospheres*, 104, 15963–15974,
970 <https://doi.org/10.1029/1999JD900144>, 1999.
- 971 Fischer, E. V., Jacob, D. J., Yantosca, R. M., Sulprizio, M. P., Millet, D. B., Mao, J., Paulot, F., Singh, H. B., Roiger,
972 A., Ries, L., Talbot, R. W., Dzepina, K., and Pandey Deolal, S.: Atmospheric peroxyacetyl nitrate (PAN): a global
973 budget and source attribution, *Atmospheric Chem. Phys.*, 14, 2679–2698, <https://doi.org/10.5194/acp-14-2679-2014>,
974 2014.
- 975 Fruekilde, P., Hjorth, J., Jensen, N. R., Kotzias, D., and Larsen, B.: OZONOLYSIS AT VEGETATION SURFACES:
976 A SOURCE OF ACETONE, 4-OXOPENTANAL, 6-METHYL-5-HEPTEN-2-ONE, AND GERANYL ACETONE
977 IN THE TROPOSPHERE, *Atmos. Environ.*, Vol. 32, No. 11, 1893–1902, 1998.
- 978 Fuentes, J. D., Gerken, T., Chamecki, M., Stoy, P., Freire, L., and Ruiz-Plancarte, J.: Turbulent transport and reactions
979 of plant-emitted hydrocarbons in an Amazonian rain forest, *Atmos. Environ.*, 279, 119094,
980 <https://doi.org/10.1016/j.atmosenv.2022.119094>, 2022.
- 981 Gouinguéné, S. P. and Turlings, T. C. J.: The Effects of Abiotic Factors on Induced Volatile Emissions in Corn Plants,
982 *Plant Physiol.*, 129, 1296–1307, <https://doi.org/10.1104/pp.001941>, 2002.

- 983 de Gouw, J. and Warneke, C.: Measurements of volatile organic compounds in the earth's atmosphere using proton-
984 transfer-reaction mass spectrometry, *Mass Spectrom. Rev.*, 26, 223–257, <https://doi.org/10.1002/mas.20119>, 2007.
- 985 Guenther, A.: Natural emissions of non-methane volatile organic compounds, carbon monoxide, and oxides of
986 nitrogen from North America, *Atmos. Environ.*, 34, 2205–2230, [https://doi.org/10.1016/S1352-2310\(99\)00465-3](https://doi.org/10.1016/S1352-2310(99)00465-3),
987 2000.
- 988 Guenther, A.: Biological and Chemical Diversity of Biogenic Volatile Organic Emissions into the Atmosphere, *Int.*
989 *Sch. Res. Not.*, 2013, e786290, <https://doi.org/10.1155/2013/786290>, 2013.
- 990 Guimbaud, C., Catoire, V., Bergeat, A., Michel, E., Schoon, N., Amelynck, C., Labonnette, D., and Poulet, G.:
991 Kinetics of the reactions of acetone and glyoxal with O₂⁺ and NO⁺ ions and application to the detection of oxygenated
992 volatile organic compounds in the atmosphere by chemical ionization mass spectrometry, *Int. J. Mass Spectrom.*, 263,
993 276–288, <https://doi.org/10.1016/j.ijms.2007.03.006>, 2007.
- 994 He, J., Halitschke, R., Schuman, M. C., and Baldwin, I. T.: Light dominates the diurnal emissions of herbivore-induced
995 volatiles in wild tobacco, *BMC Plant Biol.*, 21, 401, <https://doi.org/10.1186/s12870-021-03179-z>, 2021.
- 996 Heiden, A. C., Kobel, K., Komenda, M., Koppmann, R., Shao, M., and Wildt, J.: Toluene emissions from plants,
997 *Geophys. Res. Lett.*, 26, 1283–1286, <https://doi.org/10.1029/1999GL900220>, 1999.
- 998 Hellén, H., Hakola, H., Reissell, A., and Ruuskanen, T. M.: Carbonyl compounds in boreal coniferous forest air in
999 Hyttiälä, Southern Finland, *Atmospheric Chem. Phys.*, 4, 1771–1780, <https://doi.org/10.5194/acp-4-1771-2004>,
1000 2004.
- 1001 Holanda, B. A., Pöhlker, M. L., Walter, D., Saturno, J., Sörgel, M., Ditas, J., Ditas, F., Schulz, C., Franco, M. A.,
1002 Wang, Q., Donth, T., Artaxo, P., Barbosa, H. M. J., Borrmann, S., Braga, R., Brito, J., Cheng, Y., Dollner, M., Kaiser,
1003 J. W., Klimach, T., Knote, C., Krüger, O. O., Fütterer, D., Lavrič, J. V., Ma, N., Machado, L. A. T., Ming, J., Morais,
1004 F. G., Paulsen, H., Sauer, D., Schlager, H., Schneider, J., Su, H., Weinzierl, B., Walser, A., Wendisch, M., Ziereis, H.,
1005 Zöger, M., Pöschl, U., Andreae, M. O., and Pöhlker, C.: Influx of African biomass burning aerosol during the
1006 Amazonian dry season through layered transatlantic transport of black carbon-rich smoke, *Atmospheric Chem. Phys.*,
1007 20, 4757–4785, <https://doi.org/10.5194/acp-20-4757-2020>, 2020.
- 1008 Holanda, B. A., Franco, M. A., Walter, D., Artaxo, P., Carbone, S., Cheng, Y., Chowdhury, S., Ditas, F., Gysel-Ber,
1009 M., Klimach, T., Kremper, L. A., Krüger, O. O., Lavric, J. V., Lelieveld, J., Ma, C., Machado, L. A. T., Modini, R.
1010 L., Morais, F. G., Pozzer, A., Saturno, J., Su, H., Wendisch, M., Wolff, S., Pöhlker, M. L., Andreae, M. O., Pöschl,
1011 U., and Pöhlker, C.: African biomass burning affects aerosol cycling over the Amazon, *Commun. Earth Environ.*, 4,
1012 1–15, <https://doi.org/10.1038/s43247-023-00795-5>, 2023.
- 1013 Holzinger, R., Sandoval-Soto, L., Rottenberger, S., Crutzen, P. J., and Kesselmeier, J.: Emissions of volatile organic
1014 compounds from *Quercus ilex* L. measured by Proton Transfer Reaction Mass Spectrometry under different
1015 environmental conditions, *J. Geophys. Res. Atmospheres*, 105, 20573–20579, <https://doi.org/10.1029/2000JD900296>,
1016 2000.
- 1017 Holzinger, R., Lee, A., Paw, K. T., and Goldstein, U. a. H.: Observations of oxidation products above a forest imply
1018 biogenic emissions of very reactive compounds, *Atmospheric Chem. Phys.*, 5, 67–75, <https://doi.org/10.5194/acp-5-67-2005>, 2005.
- 1020 Hunter, E. P. L. and Lias, S. G.: Evaluated Gas Phase Basicities and Proton Affinities of Molecules: An Update, *J.*
1021 *Phys. Chem. Ref. Data*, 27, 413–656, <https://doi.org/10.1063/1.556018>, 1998.
- 1022 Isidorov, V. A., Zenkevich, I. G., and Ioffe, B. V.: Volatile organic compounds in the atmosphere of forests,
1023 *Atmospheric Environ.* 1967, 19, 1–8, [https://doi.org/10.1016/0004-6981\(85\)90131-3](https://doi.org/10.1016/0004-6981(85)90131-3), 1985.

- 1024 Jacob, D. J., Field, B. D., Jin, E. M., Bey, I., Li, Q., Logan, J. A., Yantosca, R. M., and Singh, H. B.: Atmospheric
1025 budget of acetone, *J. Geophys. Res. Atmospheres*, 107, ACH 5-1-ACH 5-17, <https://doi.org/10.1029/2001JD000694>,
1026 2002.
- 1027 Jan, R., Asaf, S., Numan, M., Lubna, and Kim, K.-M.: Plant Secondary Metabolite Biosynthesis and Transcriptional
1028 Regulation in Response to Biotic and Abiotic Stress Conditions, *Agronomy*, 11, 968,
1029 <https://doi.org/10.3390/agronomy11050968>, 2021.
- 1030 Jardine, K., Barron-Gafford, G. A., Norman, J. P., Abrell, L., Monson, R. K., Meyers, K. T., Pavao-Zuckerman, M.,
1031 Dontsova, K., Kleist, E., Werner, C., and Huxman, T. E.: Green leaf volatiles and oxygenated metabolite emission
1032 bursts from mesquite branches following light–dark transitions, *Photosynth. Res.*, 113, 321–333,
1033 <https://doi.org/10.1007/s11120-012-9746-5>, 2012a.
- 1034 Jardine, K. J., Monson, R. K., Abrell, L., Saleska, S. R., Arneth, A., Jardine, A., Ishida, F. Y., Serrano, A. M. Y.,
1035 Artaxo, P., Karl, T., Fares, S., Goldstein, A., Loreto, F., and Huxman, T.: Within-plant isoprene oxidation confirmed
1036 by direct emissions of oxidation products methyl vinyl ketone and methacrolein, *Glob. Change Biol.*, 18, 973–984,
1037 <https://doi.org/10.1111/j.1365-2486.2011.02610.x>, 2012b.
- 1038 Jardine, K. J., Meyers, K., Abrell, L., Alves, E. G., Yanez Serrano, A. M., Kesselmeier, J., Karl, T., Guenther, A.,
1039 Vickers, C., and Chambers, J. Q.: Emissions of putative isoprene oxidation products from mango branches under
1040 abiotic stress, *J. Exp. Bot.*, 64, 3669–3679, <https://doi.org/10.1093/jxb/ert202>, 2013.
- 1041 Jardine, K. J., Chambers, J. Q., Holm, J., Jardine, A. B., Fontes, C. G., Zorzanelli, R. F., Meyers, K. T., De Souza, V.
1042 F., Garcia, S., Gimenez, B. O., Piva, L. R. de O., Higuchi, N., Artaxo, P., Martin, S., and Manzi, A. O.: Green Leaf
1043 Volatile Emissions during High Temperature and Drought Stress in a Central Amazon Rainforest, *Plants*, 4, 678–690,
1044 <https://doi.org/10.3390/plants4030678>, 2015.
- 1045 Jiménez, E., Lanza, B., Martínez, E., and Albaladejo, J.: Daytime tropospheric loss of hexanal and *trans*-2-
1046 hexenal: OH kinetics and UV photolysis, *Atmospheric Chem. Phys.*, 7, 1565–1574, [https://doi.org/10.5194/acp-7-](https://doi.org/10.5194/acp-7-1565-2007)
1047 1565-2007, 2007.
- 1048 Jordan, A., Haidacher, S., Hanel, G., Hartungen, E., Märk, L., Seehauser, H., Schotchkowsky, R., Sulzer, P., and Märk,
1049 T. D.: A high resolution and high sensitivity proton-transfer-reaction time-of-flight mass spectrometer (PTR-TOF-
1050 MS), *Int. J. Mass Spectrom.*, 286, 122–128, <https://doi.org/10.1016/j.ijms.2009.07.005>, 2009.
- 1051 Jordi Vilà-Guerau de Arellano, C. C. van H., Bart J. H. van Stratum, and Kees van den Dries: *Atmospheric Boundary
1052 Layer*, Cambridge University Press, 2015.
- 1053 Kalalian, C., Abis, L., Depoorter, A., Lunardelli, B., Perrier, S., and George, C.: Influence of indoor chemistry on the
1054 emission of mVOCs from *Aspergillus niger* molds, *Sci. Total Environ.*, 741, 140148,
1055 <https://doi.org/10.1016/j.scitotenv.2020.140148>, 2020.
- 1056 Karl, T., Guenther, A., Spirig, C., Hansel, A., and Fall, R.: Seasonal variation of biogenic VOC emissions above a
1057 mixed hardwood forest in northern Michigan, *Geophys. Res. Lett.*, 30, <https://doi.org/10.1029/2003GL018432>, 2003.
- 1058 Karl, T., Potosnak, M., Guenther, A., Clark, D., Walker, J., Herrick, J. D., and Geron, C.: Exchange processes of
1059 volatile organic compounds above a tropical rain forest: Implications for modeling tropospheric chemistry above dense
1060 vegetation, *J. Geophys. Res. Atmospheres*, 109, <https://doi.org/10.1029/2004JD004738>, 2004.
- 1061 Karl, T., Hansel, A., Cappellin, L., Kaser, L., Herdlinger-Blatt, I., and Jud, W.: Selective measurements of isoprene
1062 and 2-methyl-3-buten-2-ol based on NO⁺ and O⁺ ionization mass spectrometry, *Atmospheric Chem.
1063 Phys.*, 12, 11877–11884, <https://doi.org/10.5194/acp-12-11877-2012>, 2012.

- 1064 Kesselmeier, J.: Exchange of Short-Chain Oxygenated Volatile Organic Compounds (VOCs) between Plants and the
1065 Atmosphere: A Compilation of Field and Laboratory Studies, *J. Atmospheric Chem.*, 39, 219–233,
1066 <https://doi.org/10.1023/A:1010632302076>, 2001.
- 1067 Kesselmeier, J. and Staudt, M.: Biogenic Volatile Organic Compounds (VOC): An Overview on Emission, Physiology
1068 and Ecology, *J. Atmospheric Chem.*, 33, 23–88, <https://doi.org/10.1023/A:1006127516791>, 1999.
- 1069 Kesselmeier, J., Bode, K., Hofmann, U., Müller, H., Schäfer, L., Wolf, A., Ciccioli, P., Brancaleoni, E., Cecinato, A.,
1070 Frattoni, M., Foster, P., Ferrari, C., Jacob, V., Fugit, J. L., Dutaur, L., Simon, V., and Torres, L.: Emission of short
1071 chained organic acids, aldehydes and monoterpenes from *Quercus ilex* L. and *Pinus pinea* L. in relation to
1072 physiological activities, carbon budget and emission algorithms, *Atmos. Environ.*, 31, 119–133,
1073 [https://doi.org/10.1016/S1352-2310\(97\)00079-4](https://doi.org/10.1016/S1352-2310(97)00079-4), 1997.
- 1074 Kesselmeier, J., Kuhn, U., Wolf, A., Andreae, M. O., Ciccioli, P., Brancaleoni, E., Frattoni, M., Guenther, A.,
1075 Greenberg, J., De Castro Vasconcellos, P., de Oliva, T., Tavares, T., and Artaxo, P.: Atmospheric volatile organic
1076 compounds (VOC) at a remote tropical forest site in central Amazonia, *Atmos. Environ.*, 34, 4063–4072,
1077 [https://doi.org/10.1016/S1352-2310\(00\)00186-2](https://doi.org/10.1016/S1352-2310(00)00186-2), 2000.
- 1078 Khan, M. A. H., Cooke, M. C., Utembe, S. R., Archibald, A. T., Derwent, R. G., Xiao, P., Percival, C. J., Jenkin, M.
1079 E., Morris, W. C., and Shallcross, D. E.: Global modeling of the nitrate radical (NO₃) for present and pre-industrial
1080 scenarios, *Atmospheric Res.*, 164–165, 347–357, <https://doi.org/10.1016/j.atmosres.2015.06.006>, 2015.
- 1081 Kirstine, W., Galbally, I., Ye, Y., and Hooper, M.: Emissions of volatile organic compounds (primarily oxygenated
1082 species) from pasture, *J. Geophys. Res. Atmospheres*, 103, 10605–10619, <https://doi.org/10.1029/97JD03753>, 1998.
- 1083 Kirstine, W. V. and Galbally, I. E.: The global atmospheric budget of ethanol revisited, *Atmospheric Chem. Phys.*,
1084 12, 545–555, <https://doi.org/10.5194/acp-12-545-2012>, 2012.
- 1085 König, G., Brunda, M., Puxbaum, H., Hewitt, C. N., Duckham, S. C., and Rudolph, J.: Relative contribution of
1086 oxygenated hydrocarbons to the total biogenic VOC emissions of selected mid-European agricultural and natural plant
1087 species, *Atmos. Environ.*, 29, 861–874, [https://doi.org/10.1016/1352-2310\(95\)00026-U](https://doi.org/10.1016/1352-2310(95)00026-U), 1995.
- 1088 Koss, A. R., Warneke, C., Yuan, B., Coggon, M. M., Veres, P. R., and de Gouw, J. A.: Evaluation of
1089 NO₃ and reagent ion chemistry for online measurements of atmospheric volatile organic
1090 compounds, *Atmospheric Meas. Tech.*, 9, 2909–2925, <https://doi.org/10.5194/amt-9-2909-2016>, 2016.
- 1091 Kreuzwieser, J., Kühnemann, F., Martis, A., Rennenberg, H., and Urban, W.: Diurnal pattern of acetaldehyde emission
1092 by flooded poplar trees, *Physiol. Plant.*, 108, 79–86, <https://doi.org/10.1034/j.1399-3054.2000.108001079.x>, 2000.
- 1093 Kuhn, U., Rottenberger, S., Biesenthal, T., Wolf, A., Schebeske, G., Ciccioli, P., Brancaleoni, E., Frattoni, M.,
1094 Tavares, T. M., and Kesselmeier, J.: Seasonal differences in isoprene and light-dependent monoterpene emission by
1095 Amazonian tree species, *Glob. Change Biol.*, 10, 663–682, <https://doi.org/10.1111/j.1529-8817.2003.00771.x>, 2004a.
- 1096 Kuhn, U., Rottenberger, S., Biesenthal, T., Wolf, A., Schebeske, G., Ciccioli, P., and Kesselmeier, J.: Strong
1097 correlation between isoprene emission and gross photosynthetic capacity during leaf phenology of the tropical tree
1098 species *Hymenaea courbaril* with fundamental changes in volatile organic compounds emission composition during
1099 early leaf development, *Plant Cell Environ.*, 27, 1469–1485, <https://doi.org/10.1111/j.1365-3040.2004.01252.x>,
1100 2004b.
- 1101 Kuhn, U., Andreae, M. O., Ammann, C., Araújo, A. C., Brancaleoni, E., Ciccioli, P., Dindorf, T., Frattoni, M., Gatti,
1102 L. V., Ganzeveld, L., Kruijt, B., Lelieveld, J., Lloyd, J., Meixner, F. X., Nobre, A. D., Pöschl, U., Spirig, C., Stefani,
1103 P., Thielmann, A., Valentini, R., and Kesselmeier, J.: Isoprene and monoterpene fluxes from Central Amazonian
1104 rainforest inferred from tower-based and airborne measurements, and implications on the atmospheric chemistry and
1105 the local carbon budget, *Atmospheric Chem. Phys.*, 7, 2855–2879, <https://doi.org/10.5194/acp-7-2855-2007>, 2007.

- 1106 Ladino-Orjuela, G., Gomes, E., da Silva, R., Salt, C., and Parsons, J. R.: Metabolic Pathways for Degradation of
 1107 Aromatic Hydrocarbons by Bacteria, in: *Reviews of Environmental Contamination and Toxicology Volume 237*, vol.
 1108 237, edited by: de Voogt, W. P., Springer International Publishing, Cham, 105–121, [https://doi.org/10.1007/978-3-](https://doi.org/10.1007/978-3-319-23573-8_5)
 1109 319-23573-8_5, 2016.
- 1110 Langford, B., Misztal, P. K., Nemitz, E., Davison, B., Helfter, C., Pugh, T. a. M., MacKenzie, A. R., Lim, S. F., and
 1111 Hewitt, C. N.: Fluxes and concentrations of volatile organic compounds from a South-East Asian tropical rainforest,
 1112 *Atmospheric Chem. Phys.*, 10, 8391–8412, <https://doi.org/10.5194/acp-10-8391-2010>, 2010.
- 1113 Laothawornkitkul, J., Taylor, J. E., Paul, N. D., and Hewitt, C. N.: Biogenic volatile organic compounds in the Earth
 1114 system, *New Phytol.*, 183, 27–51, <https://doi.org/10.1111/j.1469-8137.2009.02859.x>, 2009.
- 1115 Lary, D. J. and Shallcross, D. E.: Central role of carbonyl compounds in atmospheric chemistry, *J. Geophys. Res.*
 1116 *Atmospheres*, 105, 19771–19778, <https://doi.org/10.1029/1999JD901184>, 2000.
- 1117 Lelieveld, J., Gromov, S., Pozzer, A., and Taraborrelli, D.: Global tropospheric hydroxyl distribution, budget and
 1118 reactivity, *Atmospheric Chem. Phys.*, 16, 12477–12493, <https://doi.org/10.5194/acp-16-12477-2016>, 2016.
- 1119 Lewis, H. L.: Caproic Acid Metabolism and the Production of 2-Pentanone and Gluconic Acid by *Aspergillus niger*,
 1120 *Microbiology*, 63, 203–210, <https://doi.org/10.1099/00221287-63-2-203>, 1970.
- 1121 Li, X.-B., Zhang, C., Liu, A., Yuan, B., Yang, H., Liu, C., Wang, S., Huangfu, Y., Qi, J., Liu, Z., He, X., Song, X.,
 1122 Chen, Y., Peng, Y., Zhang, X., Zheng, E., Yang, L., Yang, Q., Qin, G., Zhou, J., and Shao, M.: Assessment of long
 1123 tubing in measuring atmospheric trace gases: applications on tall towers, *Environ. Sci. Atmospheres*, 3, 506–520,
 1124 <https://doi.org/10.1039/D2EA00110A>, 2023.
- 1125 Liu, Q., Gao, Y., Huang, W., Ling, Z., Wang, Z., and Wang, X.: Carbonyl compounds in the atmosphere: A review
 1126 of abundance, source and their contributions to O₃ and SOA formation, *Atmospheric Res.*, 274, 106184,
 1127 <https://doi.org/10.1016/j.atmosres.2022.106184>, 2022.
- 1128 Liu, Y., Brito, J., Dorris, M. R., Rivera-Rios, J. C., Seco, R., Bates, K. H., Artaxo, P., Duvoisin, S., Keutsch, F. N.,
 1129 Kim, S., Goldstein, A. H., Guenther, A. B., Manzi, A. O., Souza, R. A. F., Springston, S. R., Watson, T. B., McKinney,
 1130 K. A., and Martin, S. T.: Isoprene photochemistry over the Amazon rainforest, *Proc. Natl. Acad. Sci.*, 113, 6125–
 1131 6130, <https://doi.org/10.1073/pnas.1524136113>, 2016.
- 1132 Matsui, K., Sugimoto, K., Kakumyan, P., Khorobrykh, S. A., and Mano, J.: Volatile Oxylipins and Related
 1133 Compounds Formed Under Stress in Plants, in: *Lipidomics: Volume 2: Methods and Protocols*, edited by: Armstrong,
 1134 D., Humana Press, Totowa, NJ, 17–28, https://doi.org/10.1007/978-1-60761-325-1_2, 2010.
- 1135 Mellouki, A., Wallington, T. J., and Chen, J.: Atmospheric Chemistry of Oxygenated Volatile Organic Compounds:
 1136 Impacts on Air Quality and Climate, *Chem. Rev.*, 115, 3984–4014, <https://doi.org/10.1021/cr500549n>, 2015.
- 1137 Mumm, R. and Dicke, M.: Variation in natural plant products and the attraction of bodyguards involved in indirect
 1138 plant defense, *Can. J. Zool.*, 88, 628–667, <https://doi.org/10.1139/Z10-032>, 2010.
- 1139 Nguyen, T. B., Crouse, J. D., Teng, A. P., St. Clair, J. M., Paulot, F., Wolfe, G. M., and Wennberg, P. O.: Rapid
 1140 deposition of oxidized biogenic compounds to a temperate forest, *Proc. Natl. Acad. Sci.*, 112, E392–E401,
 1141 <https://doi.org/10.1073/pnas.1418702112>, 2015.
- 1142 Niinemets, Ü., Fares, S., Harley, P., and Jardine, K. J.: Bidirectional exchange of biogenic volatiles with vegetation:
 1143 emission sources, reactions, breakdown and deposition, *Plant Cell Environ.*, 37, 1790–1809,
 1144 <https://doi.org/10.1111/pce.12322>, 2014.

- 1145 Orzechowska, G. E., Nguyen, H. T., and Paulson, S. E.: Photochemical Sources of Organic Acids. 2. Formation of
1146 C5–C9 Carboxylic Acids from Alkene Ozonolysis under Dry and Humid Conditions, *J. Phys. Chem. A*, 109, 5366–
1147 5375, <https://doi.org/10.1021/jp050167k>, 2005.
- 1148 Pagonis, D., Krechmer, J. E., de Gouw, J., Jimenez, J. L., and Ziemann, P. J.: Effects of gas–wall partitioning in Teflon
1149 tubing and instrumentation on time-resolved measurements of gas-phase organic compounds, *Atmospheric Meas.*
1150 *Tech.*, 10, 4687–4696, <https://doi.org/10.5194/amt-10-4687-2017>, 2017.
- 1151 Parolin, P., De Simone, O., Haase, K., Waldhoff, D., Rottenberger, S., Kuhn, U., Kesselmeier, J., Kleiss, B., Schmidt,
1152 W., Pledade, M. T. F., and Junk, W. J.: Central Amazonian floodplain forests: Tree adaptations in a pulsing system,
1153 *Bot. Rev.*, 70, 357–380, [https://doi.org/10.1663/0006-8101\(2004\)070\[0357:CAFFTA\]2.0.CO;2](https://doi.org/10.1663/0006-8101(2004)070[0357:CAFFTA]2.0.CO;2), 2004.
- 1154 Pfannerstill, E. Y., Reijrink, N. G., Edtbauer, A., Ringsdorf, A., Zannoni, N., Araújo, A., Ditas, F., Holanda, B. A.,
1155 Sá, M. O., Tsokankunku, A., Walter, D., Wolff, S., Lavrič, J. V., Pöhlker, C., Sörgel, M., and Williams, J.: Total OH
1156 reactivity over the Amazon rainforest: variability with temperature, wind, rain, altitude, time of day, season, and an
1157 overall budget closure, *Atmospheric Chem. Phys.*, 21, 6231–6256, <https://doi.org/10.5194/acp-21-6231-2021>, 2021.
- 1158 Pöhlker, C., Walter, D., Paulsen, H., Könemann, T., Rodríguez-Caballero, E., Moran-Zuloaga, D., Brito, J., Carbone,
1159 S., Degrendele, C., Després, V. R., Ditas, F., Holanda, B. A., Kaiser, J. W., Lammel, G., Lavrič, J. V., Jing, M.,
1160 Pickersgill, D., Pöhlker, M. L., Praß, M., Löbs, N., Saturno, J., Sörgel, M., Wang, Q., Weber, B., Wolff, S., Artaxo,
1161 P., Pöschl, U., and Andreae, M. O.: Land cover and its transformation in the backward trajectory footprint region of
1162 the Amazon Tall Tower Observatory, *Atmospheric Chem. Phys.*, 19, 8425–8470, <https://doi.org/10.5194/acp-19-8425-2019>, 2019.
- 1164 Prather, M. J. and Jacob, D. J.: A persistent imbalance in HO_x and NO_x photochemistry of the upper troposphere
1165 driven by deep tropical convection, *Geophys. Res. Lett.*, 24, 3189–3192, <https://doi.org/10.1029/97GL03027>, 1997.
- 1166 Restrepo-Coupe, N., da Rocha, H. R., Hutyra, L. R., da Araujo, A. C., Borma, L. S., Christoffersen, B., Cabral, O. M.
1167 R., de Camargo, P. B., Cardoso, F. L., da Costa, A. C. L., Fitzjarrald, D. R., Goulden, M. L., Kruijt, B., Maia, J. M.
1168 F., Malhi, Y. S., Manzi, A. O., Miller, S. D., Nobre, A. D., von Randow, C., Sá, L. D. A., Sakai, R. K., Tota, J., Wofsy,
1169 S. C., Zanchi, F. B., and Saleska, S. R.: What drives the seasonality of photosynthesis across the Amazon basin? A
1170 cross-site analysis of eddy flux tower measurements from the Brasil flux network, *Agric. For. Meteorol.*, 182–183,
1171 128–144, <https://doi.org/10.1016/j.agrformet.2013.04.031>, 2013.
- 1172 Ringsdorf, A., Edtbauer, A., Vilà-Guerau de Arellano, J., Pfannerstill, E. Y., Gromov, S., Kumar, V., Pozzer, A.,
1173 Wolff, S., Tsokankunku, A., Soergel, M., Sá, M. O., Araújo, A., Ditas, F., Poehlker, C., Lelieveld, J., and Williams,
1174 J.: Inferring the diurnal variability of OH radical concentrations over the Amazon from BVOC measurements, *Sci.*
1175 *Rep.*, 13, 14900, <https://doi.org/10.1038/s41598-023-41748-4>, 2023.
- 1176 Rivera-Rios, J. C., Nguyen, T. B., Crouse, J. D., Jud, W., St. Clair, J. M., Mikoviny, T., Gilman, J. B., Lerner, B. M.,
1177 Kaiser, J. B., Gouw, J., Wisthaler, A., Hansel, A., Wennberg, P. O., Seinfeld, J. H., and Keutsch, F. N.: Conversion
1178 of hydroperoxides to carbonyls in field and laboratory instrumentation: Observational bias in diagnosing pristine
1179 versus anthropogenically controlled atmospheric chemistry, *Geophys. Res. Lett.*, 41, 8645–8651,
1180 <https://doi.org/10.1002/2014GL061919>, 2014.
- 1181 Roberts, J. M: PAN and Related Compounds, in: *Volatile Organic Compounds in the Atmosphere*, Blackwell
1182 Publishing Ltd, 2007.
- 1183 Romano, A. and Hanna, G. B.: Identification and quantification of VOCs by proton transfer reaction time of flight
1184 mass spectrometry: An experimental workflow for the optimization of specificity, sensitivity, and accuracy, *J. Mass*
1185 *Spectrom.*, 53, 287–295, <https://doi.org/10.1002/jms.4063>, 2018.
- 1186 Rottenberger, S., Kuhn, U., Wolf, A., Schebeske, G., Oliva, S. T., Tavares, T. M., and Kesselmeier, J.: Exchange of
1187 Short-Chain Aldehydes Between Amazonian Vegetation and the Atmosphere, *Ecol. Appl.*, 14, 247–262,
1188 <https://doi.org/10.1890/01-6027>, 2004.

- 1189 Rottenberger, S., Kleiss, B., Kuhn, U., Wolf, A., Piedade, M. T. F., Junk, W., and Kesselmeier, J.: The effect of
1190 flooding on the exchange of the volatile C₂-compounds ethanol, acetaldehyde and acetic acid between leaves of
1191 Amazonian floodplain tree species and the atmosphere, *Biogeosciences*, 5, 1085–1100, [https://doi.org/10.5194/bg-5-](https://doi.org/10.5194/bg-5-1085-2008)
1192 1085-2008, 2008.
- 1193 Rummel, U., Ammann, C., Gut, A., Meixner, F. X., and Andreae, M. O.: Eddy covariance measurements of nitric
1194 oxide flux within an Amazonian rain forest, *J. Geophys. Res. Atmospheres*, 107, LBA 17-1-LBA 17-9,
1195 <https://doi.org/10.1029/2001JD000520>, 2002.
- 1196 Scala, A., Allmann, S., Mirabella, R., Haring, M. A., and Schuurink, R. C.: Green Leaf Volatiles: A Plant's
1197 Multifunctional Weapon against Herbivores and Pathogens, *Int. J. Mol. Sci.*, 14, 17781–17811,
1198 <https://doi.org/10.3390/ijms140917781>, 2013.
- 1199 Schade, G. W. and Goldstein, A. H.: Fluxes of oxygenated volatile organic compounds from a ponderosa pine
1200 plantation, *J. Geophys. Res. Atmospheres*, 106, 3111–3123, <https://doi.org/10.1029/2000JD900592>, 2001.
- 1201 Sebbar, N., Bozzelli, J. W., and Bockhorn, H.: Thermochemistry and Reaction Paths in the Oxidation Reaction of
1202 Benzoyl Radical: C₆H₅C•(=O), *J. Phys. Chem. A*, 115, 11897–11914, <https://doi.org/10.1021/jp2078067>, 2011.
- 1203 Seco, R., Peñuelas, J., and Filella, I.: Short-chain oxygenated VOCs: Emission and uptake by plants and atmospheric
1204 sources, sinks, and concentrations, *Atmos. Environ.*, 41, 2477–2499, <https://doi.org/10.1016/j.atmosenv.2006.11.029>,
1205 2007.
- 1206 Singh, H. B., Herlth, D., O'Hara, D., Salas, L., Torres, A. L., Gregory, G. L., Sachse, G. W., and Kasting, J. F.:
1207 Atmospheric peroxyacetyl nitrate measurements over the Brazilian Amazon Basin during the wet season:
1208 Relationships with nitrogen oxides and ozone, *J. Geophys. Res. Atmospheres*, 95, 16945–16954,
1209 <https://doi.org/10.1029/JD095iD10p16945>, 1990.
- 1210 Singh, H. B., Salas, L. J., Chatfield, R. B., Czech, E., Fried, A., Walega, J., Evans, M. J., Field, B. D., Jacob, D. J.,
1211 Blake, D., Heikes, B., Talbot, R., Sachse, G., Crawford, J. H., Avery, M. A., Sandholm, S., and Fuelberg, H.: Analysis
1212 of the atmospheric distribution, sources, and sinks of oxygenated volatile organic chemicals based on measurements
1213 over the Pacific during TRACE-P, *J. Geophys. Res. Atmospheres*, 109, <https://doi.org/10.1029/2003JD003883>, 2004.
- 1214 Smith, D., Wang, T., and Španěl, P.: Analysis of ketones by selected ion flow tube mass spectrometry, *Rapid Commun.*
1215 *Mass Spectrom.*, 17, 2655–2660, <https://doi.org/10.1002/rcm.1244>, 2003.
- 1216 Smith, D., Chippendale, T. W. E., and Španěl, P.: Selected ion flow tube, SIFT, studies of the reactions of H₃O⁺,
1217 NO⁺ and O₂⁺ with some biologically active isobaric compounds in preparation for SIFT-MS analyses, *Int. J. Mass*
1218 *Spectrom.*, 303, 81–89, <https://doi.org/10.1016/j.ijms.2011.01.005>, 2011.
- 1219 Španěl, P. and Smith, D.: SIFT studies of the reactions of H₃O⁺, NO⁺ and O₂⁺ with a series of volatile carboxylic
1220 acids and esters, *Int. J. Mass Spectrom. Ion Process.*, 172, 137–147, [https://doi.org/10.1016/S0168-1176\(97\)00246-2](https://doi.org/10.1016/S0168-1176(97)00246-2),
1221 1998.
- 1222 Španěl, P. and Smith, D.: SIFT studies of the reactions of H₃O⁺, NO⁺ and O₂⁺ with several ethers, *Int. J. Mass*
1223 *Spectrom. Ion Process.*, 172, 239–247, [https://doi.org/10.1016/S0168-1176\(97\)00277-2](https://doi.org/10.1016/S0168-1176(97)00277-2), 1998.
- 1224 Španěl, P., Ji, Y., and Smith, D.: SIFT studies of the reactions of H₃O⁺, NO⁺ and O₂⁺ with a series of aldehydes and
1225 ketones, *Int. J. Mass Spectrom. Ion Process.*, 165–166, 25–37, [https://doi.org/10.1016/S0168-1176\(97\)00166-3](https://doi.org/10.1016/S0168-1176(97)00166-3), 1997.
- 1226 Španěl, P., Wang, T., and Smith, D.: A selected ion flow tube, SIFT, study of the reactions of H₃O⁺, NO⁺ and O₂⁺
1227 ions with a series of diols, *Int. J. Mass Spectrom.*, 218, 227–236, [https://doi.org/10.1016/S1387-3806\(02\)00724-8](https://doi.org/10.1016/S1387-3806(02)00724-8),
1228 2002.

- 1229 Tani, A. and Hewitt, C. N.: Uptake of Aldehydes and Ketones at Typical Indoor Concentrations by Houseplants,
1230 Environ. Sci. Technol., 43, 8338–8343, <https://doi.org/10.1021/es9020316>, 2009.
- 1231 Tani, A., Tobe, S., and Shimizu, S.: Uptake of Methacrolein and Methyl Vinyl Ketone by Tree Saplings and
1232 Implications for Forest Atmosphere, Environ. Sci. Technol., 44, 7096–7101, <https://doi.org/10.1021/es1017569>, 2010.
- 1233 Tani, A., Tobe, S., and Shimizu, S.: Leaf uptake of methyl ethyl ketone and croton aldehyde by *Castanopsis sieboldii*
1234 and *Viburnum odoratissimum* saplings, Atmos. Environ., 70, 300–306,
1235 <https://doi.org/10.1016/j.atmosenv.2012.12.043>, 2013.
- 1236 Trebs, I., Mayol-Bracero, O. L., Pauliquevis, T., Kuhn, U., Sander, R., Ganzeveld, L., Meixner, F. X., Kesselmeier,
1237 J., Artaxo, P., and Andreae, M. O.: Impact of the Manaus urban plume on trace gas mixing ratios near the surface in
1238 the Amazon Basin: Implications for the NO-NO₂-O₃ photostationary state and peroxy radical levels, J. Geophys. Res.
1239 Atmospheres, 117, <https://doi.org/10.1029/2011JD016386>, 2012.
- 1240 Villanueva, F., Tapia, A., Notario, A., Albaladejo, J., and Martínez, E.: Ambient levels and temporal trends of VOCs,
1241 including carbonyl compounds, and ozone at Cabañeros National Park border, Spain, Atmos. Environ., 85, 256–265,
1242 <https://doi.org/10.1016/j.atmosenv.2013.12.015>, 2014.
- 1243 Villanueva-Fierro, I., Popp, C. J., and Martin, R. S.: Biogenic emissions and ambient concentrations of hydrocarbons,
1244 carbonyl compounds and organic acids from ponderosa pine and cottonwood trees at rural and forested sites in Central
1245 New Mexico, Atmos. Environ., 38, 249–260, <https://doi.org/10.1016/j.atmosenv.2003.09.051>, 2004.
- 1246 Wang, C., Yuan, B., Wu, C., Wang, S., Qi, J., Wang, B., Wang, Z., Hu, W., Chen, W., Ye, C., Wang, W., Sun, Y.,
1247 Wang, C., Huang, S., Song, W., Wang, X., Yang, S., Zhang, S., Xu, W., Ma, N., Zhang, Z., Jiang, B., Su, H., Cheng,
1248 Y., Wang, X., and Shao, M.: Measurements of higher alkanes using NO⁺ and chemical ionization
1249 in PTR-ToF-MS: important contributions of higher alkanes to secondary organic aerosols in China, Atmospheric
1250 Chem. Phys., 20, 14123–14138, <https://doi.org/10.5194/acp-20-14123-2020>, 2020a.
- 1251 Wang, M., Zhang, L., Boo, K. H., Park, E., Drakakaki, G., and Zakharov, F.: PDC1, a pyruvate/ α -ketoacid
1252 decarboxylase, is involved in acetaldehyde, propanal and pentanal biosynthesis in melon (*Cucumis melo* L.) fruit,
1253 Plant J., 98, 112–125, <https://doi.org/10.1111/tpj.14204>, 2019.
- 1254 Wang, N., Edtbauer, A., Stöner, C., Pozzer, A., Bourtsoukidis, E., Ernle, L., Dienhart, D., Hottmann, B., Fischer, H.,
1255 Schuladen, J., Crowley, J. N., Paris, J.-D., Lelieveld, J., and Williams, J.: Measurements of carbonyl compounds
1256 around the Arabian Peninsula indicate large missing sources of acetaldehyde, Gases/Field
1257 Measurements/Troposphere/Chemistry (chemical composition and reactions), <https://doi.org/10.5194/acp-2020-135>,
1258 2020b.
- 1259 Warneck, P.; Williams, J.: The Atmospheric Chemists Companion, 1., Springer Verlag GmbH, 2012.
- 1260 Warneke, C., Karl, T., Judmaier, H., Hansel, A., Jordan, A., Lindinger, W., and Crutzen, P. J.: Acetone, methanol,
1261 and other partially oxidized volatile organic emissions from dead plant matter by abiological processes: Significance
1262 for atmospheric HO_x chemistry, Glob. Biogeochem. Cycles, 13, 9–17, <https://doi.org/10.1029/98GB02428>, 1999.
- 1263 Williams, J., Fischer, H., Harris, G. W., Crutzen, P. J., Hoor, P., Hansel, A., Holzinger, R., Warneke, C., Lindinger,
1264 W., Scheeren, B., and Lelieveld, J.: Variability-lifetime relationship for organic trace gases: A novel aid to compound
1265 identification and estimation of HO concentrations, J. Geophys. Res. Atmospheres, 105, 20473–20486,
1266 <https://doi.org/10.1029/2000JD900203>, 2000.
- 1267 Williams, J., Pöschl, U., Crutzen, P. J., Hansel, A., Holzinger, R., Warneke, C., Lindinger, W., and Lelieveld, J.: An
1268 Atmospheric Chemistry Interpretation of Mass Scans Obtained from a Proton Transfer Mass Spectrometer Flown over
1269 the Tropical Rainforest of Surinam, 2001.

- 1270 Wolfe, G. M., Thornton, J. A., McKay, M., and Goldstein, A. H.: Forest-atmosphere exchange of ozone: sensitivity
1271 to very reactive biogenic VOC emissions and implications for in-canopy photochemistry, *Atmospheric Chem. Phys.*,
1272 11, 7875–7891, <https://doi.org/10.5194/acp-11-7875-2011>, 2011.
- 1273 Xing, J.-H., Ono, M., Kuroda, A., Obi, K., Sato, K., and Imamura, T.: Kinetic Study of the Daytime Atmospheric Fate
1274 of (Z)-3-Hexenal, *J. Phys. Chem. A*, 116, 8523–8529, <https://doi.org/10.1021/jp303202h>, 2012.
- 1275 Yamauchi, Y., Kunishima, M., Mizutani, M., and Sugimoto, Y.: Reactive short-chain leaf volatiles act as powerful
1276 inducers of abiotic stress-related gene expression, *Sci. Rep.*, 5, 8030, <https://doi.org/10.1038/srep08030>, 2015.
- 1277 Yáñez-Serrano, A. M., Nölscher, A. C., Williams, J., Wolff, S., Alves, E., Martins, G. A., Bourtsoukidis, E., Brito, J.,
1278 Jardine, K., Artaxo, P., and Kesselmeier, J.: Diel and seasonal changes of biogenic volatile organic compounds within
1279 and above an Amazonian rainforest, *Atmospheric Chem. Phys.*, 15, 3359–3378, [https://doi.org/10.5194/acp-15-3359-](https://doi.org/10.5194/acp-15-3359-2015)
1280 2015, 2015.
- 1281 Yáñez-Serrano, A. M., Nölscher, A. C., Bourtsoukidis, E., Derstroff, B., Zannoni, N., Gros, V., Lanza, M., Brito, J.,
1282 Noe, S. M., House, E., Hewitt, C. N., Langford, B., Nemitz, E., Behrendt, T., Williams, J., Artaxo, P., Andreae, M.
1283 O., and Kesselmeier, J.: Atmospheric mixing ratios of methyl ethyl ketone (2-butanone) in tropical, boreal, temperate
1284 and marine environments, *Atmospheric Chem. Phys.*, 16, 10965–10984, [https://doi.org/10.5194/acp-16-10965-](https://doi.org/10.5194/acp-16-10965-2016)
1285 2016.
- 1286 Yee, L. D., Isaacman-VanWertz, G., Wernis, R. A., Meng, M., Rivera, V., Kreisberg, N. M., Hering, S. V., Bering,
1287 M. S., Glasius, M., Upshur, M. A., Gray Bé, A., Thomson, R. J., Geiger, F. M., Offenberg, J. H., Lewandowski, M.,
1288 Kourtchev, I., Kalberer, M., de Sá, S., Martin, S. T., Alexander, M. L., Palm, B. B., Hu, W., Campuzano-Jost, P., Day,
1289 D. A., Jimenez, J. L., Liu, Y., McKinney, K. A., Artaxo, P., Viegas, J., Manzi, A., Oliveira, M. B., de Souza, R.,
1290 Machado, L. A. T., Longo, K., and Goldstein, A. H.: Observations of sesquiterpenes and their oxidation products in
1291 central Amazonia during the wet and dry seasons, *Atmospheric Chem. Phys.*, 18, 10433–10457,
1292 [https://doi.org/10.5194/acp-18-10433-](https://doi.org/10.5194/acp-18-10433-2018)2018, 2018.
- 1293 Yee, L. D., Goldstein, A. H., and Kreisberg, N. M.: Investigating Secondary Aerosol Processes in the Amazon through
1294 Molecular-level Characterization of Semi-Volatile Organics, Univ. of California, Berkeley, CA (United States),
1295 <https://doi.org/10.2172/1673764>, 2020.
- 1296 Zannoni, N., Wikelski, M., Gagliardo, A., Raza, A., Kramer, S., Seghetti, C., Wang, N., Edtbauer, A., and Williams,
1297 J.: Identifying volatile organic compounds used for olfactory navigation by homing pigeons, *Sci. Rep.*, 10, 15879,
1298 [https://doi.org/10.1038/s41598-020-72525-](https://doi.org/10.1038/s41598-020-72525-2)2, 2020a.
- 1299 Zannoni, N., Leppla, D., Lembo Silveira de Assis, P. I., Hoffmann, T., Sá, M., Araújo, A., and Williams, J.: Surprising
1300 chiral composition changes over the Amazon rainforest with height, time and season, *Commun. Earth Environ.*, 1, 1–
1301 11, [https://doi.org/10.1038/s43247-020-0007-](https://doi.org/10.1038/s43247-020-0007-9)9, 2020b.
- 1302